



HHS Public Access

Author manuscript

Bioorg Med Chem. Author manuscript; available in PMC 2022 May 24.

Published in final edited form as:

Bioorg Med Chem. 2021 October 15; 48: 116414. doi:10.1016/j.bmc.2021.116414.

Design, synthesis, and antiviral activity of phenylalanine derivatives as HIV-1 capsid inhibitors

Jing Li^a, Xiangyi Jiang^a, Alexej Dick^b, Prem Prakash Sharma^c, Chin-Ho Chen^d, Brijesh Rathi^c, Dongwei Kang^a, Zhao Wang^a, Xiangkai Ji^a, Kuo-Hsiung Lee^{e,*}, Simon Cocklin^{b,*}, Xinyong Liu^{a,*}, Peng Zhan^{a,*}

^aDepartment of Medicinal Chemistry, Key Laboratory of Chemical Biology (Ministry of Education), School of Pharmaceutical Sciences, Shandong University, 44 West Culture Road, 250012 Ji'nan, Shandong, PR China

^bDepartment of Biochemistry & Molecular Biology, Drexel University College of Medicine, Philadelphia, PA 19102, USA

^cLaboratory for Translational Chemistry and Drug Discovery, Department of Chemistry, Hansraj College, University of Delhi, Delhi 110007, India

^dDuke University Medical Center, Box 2926, Surgical Oncology Research Facility, Durham, NC 27710, USA

^eNatural Products Research Laboratories, Eshelman School of Pharmacy, University of North Carolina, Chapel Hill, NC 27599, USA

Abstract

The HIV-1 Capsid (CA) is considered as a promising target for the development of potent antiviral drugs, due to its multiple roles during the viral life cycle. Herein, we report the design, synthesis, and antiviral activity evaluation of series of novel phenylalanine derivatives as HIV-1 CA protein inhibitors. Among them, 4-methoxy-*N*-methylaniline substituted phenylalanine (**II-13c**) and indolin-5-amine substituted phenylalanine (**V-25i**) displayed exceptional anti-HIV-1 activity with the EC₅₀ value of 5.14 and 2.57 μM respectively, which is slightly weaker than that of lead compound PF-74 (EC₅₀ = 0.42 μM). Besides, surface plasmon resonance (SPR) binding assay demonstrated **II-13c** and **V-25i** prefer to combine with CA hexamer rather than monomer, which is similar to PF-74. Subsequently, molecular dynamics simulation (MD) revealed potential interactions between representative compounds with HIV-1 CA hexamer. Overall, this work laid a solid foundation for further structural optimization to discover novel promising HIV-1 CA inhibitors.

*Corresponding authors. khlee@unc.edu (K.-H. Lee), sc349@drexel.edu (S. Cocklin), xinyongl@sdu.edu.cn (X. Liu), zhanpeng1982@sdu.edu.cn (P. Zhan).

Declaration of Competing Interest

The authors declare that they have no known competing financial interests or personal relationships that could have appeared to influence the work reported in this paper.

Appendix A. Supplementary material

Supplementary data to this article can be found online at <https://doi.org/10.1016/j.bmc.2021.116414>.

Keywords

HIV-1 Capside Protein; PF-74 derivative; Scaffold Hopping; HIV-1 CA inhibitors

1. Introduction

Acquired immune deficiency syndrome (AIDS), mainly caused by the human immunodeficiency virus type 1 (HIV-1), still remains a serious threat to worldwide public health¹. Although combination antiretroviral therapy (cART) could suppress the viral load and improve the life quality of the patient living with HIV, the adverse side effects and the emergence of drug resistance *etc.* restrict its application^{2,3}. Nowadays, HIV-1 infection cannot be completely cured. Consequently, it's of great significance to continue exploring novel anti-HIV-1 drugs, especially for the unexploited targets with unique mechanism⁴.

HIV-1 CA is an asymmetric fullerene-shaped cone comprised of about 1500 CA monomer, which is obtained by cutting the gag-pol precursor protein⁵. CA monomer is composed of an N-terminal domain (NTD, residues 1 to 145) and a C-terminal domain (CTD, residues 150 to 231), which are connected by a flexible linker^{6,7}. HIV-1 CA protein plays multiple roles at the early (uncoating, reverse transcription, nuclear import, integration, *etc.*) and late stages (assembly and maturation) of HIV-1 life cycle^{8,9}. At the early stage, CA protein could interact with host factors, such as cyclophilin A (CypA), nucleoporin 153 (NUP153) and CPSF6 (cleavage and polyadenylation specific factor 6), TNPO3 (transportin-3) and NUP358, promoting the process of uncoating. This is essential for viral pre-integration complex entering into the nuclear and escape from host immune surveillance¹⁰⁻¹². At the late stage, the recombinant capsid encapsulates the viral gene RNA and gag-pol precursor protein, which are essential for the release of infectious viral particles⁸. Herein, HIV-1 CA is considered as a promising but underexploited target for the development of small-molecules anti-HIV-1 drugs¹³⁻¹⁷.

Currently, a series of structurally diverse HIV-1 CA inhibitors has been identified¹⁸⁻²². Among them, PF-74 has attracted a great deal of attention and has been studied extensively²³. PF-74 consists of a phenylalanine core targeting the CA NTD, an indole ring targeting the CA CTD and a flexible linker in-between (Figure. 1a)^{5,24,25}. Phenylalanine core could form hydrogen-bond or hydrophobic interactions with Met66, Leu69, Leu56, Asn57, Asn53, Lys70 of the CA NTD, the methylindole could form hydrogen-bond with Gln63, Tyr169 and form a cation-pi interaction with Arg173 and Lys182 in the CTD of the adjacent protomer^{7,25,26}. At the early stage of HIV-1 replication, PF-74 interacts with CA competitively with host factors CPSF6 and NUP153, which disturbs viral uncoating, reverse transcription, nuclear input and integration. At the late stage, PF-74 could interfere with the normal assembly process of CA, which is extremely unfavorable for the stability of CA and the maturation of virus^{8,23,25}. However, relatively low anti-HIV-1 activity ($EC_{50} = 0.45 \mu\text{M}$) and poor metabolic stability ($t_{1/2} = 1.3 \text{ min}$) emphasized the significance of continuing to optimize it^{23,27,28}. In our preceding work, lots of structurally novel PF-74 derivatives have been discovered, but they exhibited micromolar antiviral activity (Figure. 1b)²⁹⁻³³. Consequently, the need for continuing identify potential PF-74 derivatives remains.

And it is noteworthy that the phenylalanine core is essential for the maintenance of antiviral activity. The linker region and indole substituents of PF-74, which targeting the protein–protein solvent interface, has significant potential to be further modified³⁴. In this work, we continued focusing on the indole substituents and the linker of PF-74, so as to further enrich the structure–activity relationships (SARs) at this section^{35,36}. We retained the privileged phenylalanine fragment, and then we used scaffold hopping strategy to replace the linker with 3-sulfamoylbenzoic acid, 2-sulfamoylacetic acid, 2-amino-2-oxoacetic acid, 3-aminobenzamide or 3-carbamoylbenzenesulfonyl chloride to fully explore the structure–activity relationship of linker. Finally, these key intermediates react with diverse amine fragments to obtain Series I–V respectively (Figure. 1c). As a result, Series I–V, the total of 32 phenylalanine derivatives was obtained.

Herein, we report the design, synthesis and antiviral activity evaluation of 32 novel structural phenylalanine derivatives which divided into five sub-series. Furthermore, we demonstrated that **II-13c** and **V-25i** could interact with CA by surface plasmon resonance (SPR) binding assays. In addition, molecular dynamics simulation (MD) of representative compounds **II-13c** and **V-25i** was performed to explore the binding mode of CA hexamer. Briefly, this study enriched the SARs of PF-74 derivatives, which would be useful for finding novel and potent HIV-1 CA inhibitors.

2. Results and discussion

2.1. Chemistry

As shown in Scheme 1, (*tert*-butoxycarbonyl)-L-phenylalanine (**5**) was selected as the starting material, followed by reacting with 4-methoxy-*N*-methylaniline to obtain **6**, then removal of Boc group of **6** under the trifluoroacetic acid yielded key intermediate **7**.

Subsequently, as illustrated in Scheme 2, **7** reacted with methyl 3-(chlorosulfonyl)-benzoate or methyl 2-(chlorosulfonyl)-acetate or methyl 2-chloro-2-oxoacetate or 3-nitrobenzoic acid to obtain intermediate **8**, **11**, **14** or **17**, respectively. Then **8**, **11** or **14** underwent ester hydrolysis to obtain free acids, which reacted with diverse amine fragments by using HATU and DIEA to produce target compounds (series I, II and III). Then **17** reacted with SnCl₂·2H₂O to reduce nitro to amino and subsequently, compound **18** was obtained, which could react with sulfonyl chloride substituents to generate the target compounds (**series IV**).

The synthetic route of series V is shown in Scheme 3. Firstly, **20** reacted with diverse amine fragments in the presence of TEA to obtain **21**. Then, their ester bonds were hydrolyzed to get intermediate **22**. Next, **22** or commercially available **23**, **24** reacted with **7** to gain the target products (**series V**) by using HATU and DIEA.

2.2. Biological activity

All novel PF-74 derivatives were tested for their antiviral activity and cytotoxicity in MT-4 cell which infected with HIV-1 N L4–3 Nanoluc-*sec* virus. PF-74 was selected as a positive control. The EC₅₀, evaluated by luciferase gene expression assay³⁷, CC₅₀ and SI which is the ratio of CC₅₀/EC₅₀ are described in Table 1.

The results exhibited that a lot of compounds in series **II** and **V** displayed micromolar antiviral activity, but series **I**, **III** and **IV** didn't show antiviral activity at the tested concentration (5 µg/mL). Especially for series **IV**, only the exchange of sulfone and amine positions in sulfonamide of series **V**, making them lost antiviral activity, which indicated that NTD-CTD dimer interface of CA hexamer is exceedingly sensitive to the linker of PF-74. Among series **II** and **V**, the most potent compounds are **II-13c** ($EC_{50} = 5.14 \pm 1.62 \mu\text{M}$, $CC_{50} > 9.51 \mu\text{M}$) and **V-25i** ($EC_{50} = 2.57 \pm 0.79 \mu\text{M}$, $CC_{50} > 8.55 \mu\text{M}$), which is slightly weaker than that of PF-74 ($EC_{50} = 0.42 \pm 0.11 \mu\text{M}$, $CC_{50} > 11.56 \mu\text{M}$). Besides, when making a comparison between **II and 13c** and **V-25i**, two series of compounds with identical terminal substituents showed similar antiviral activity.

As for series **II**, *p*-methoxy-*N*-methylaniline (**II-13c**, $EC_{50} = 5.14 \pm 1.62 \mu\text{M}$) is better than *p*-cyanoaniline (**II-13a**, $EC_{50} = 8.09 \pm 2.76 \mu\text{M}$). Unfortunately, while the substituents are benzothiazole (**II-13b**), 5-methoxyindoline (**II-13d**), 3,5-difluoroaniline (**II-13e**), indazole (**II-13f**) and 5-nitroindoline (**II-13 g**), these compounds lost their activity against HIV-1.

Concerning series **V**, 5-aminoindoline substituted **V-25i** ($EC_{50} = 2.57 \pm 0.79 \mu\text{M}$) has the best antiviral activity. When the substituents are piperidine (**V-25b**, $EC_{50} = 4.85 \pm 1.53 \mu\text{M}$), thiomorpholine (**V-25c**, $EC_{50} = 5.06 \pm 1.43 \mu\text{M}$) and *p*-methoxy-*N*-methylaniline (**V-25 g**, $EC_{50} = 5.27 \pm 1.65 \mu\text{M}$), compounds displayed moderate antiviral activity. In addition, the substitution of *N,N*-dimethylamine (**V-25a**) caused less antiviral activity with the EC_{50} value of $8.68 \pm 2.62 \mu\text{M}$. However, the substitution of indoline (**V-25d**), 5-methoxyindoline (**V-25e**), 5-nitroindoline (**V-25f**), 3,5-difluoroaniline (**V-25 h**) and *p*-trifluoromethylaniline (**V-25j**) lead to loss of antiviral activity at the test concentration.

In conclusion, the preliminary SARs analysis of newly designed compounds showed that the linker of PF-74 derivatives, as well as the substituents part is extremely essential for anti-HIV activities, which would be used for further explore of CTD-NTD interface.

2.3. Binding to HIV-1 CA protein

Surface plasmon resonance (SPR) analysis is employed to ascertain affinity of target compounds with capsid proteins (hexamer, monomer). The representative compounds **II-13c**, **V-25i** was chosen for assay. Similarly, PF-74 was selected as a positive control. The result is showed in Table 2 and Figure 2.

Firstly, the equilibrium dissociation constant (K_D) values of tested compounds showed that they tend to combine with CA hexamer, rather than CA monomer. In addition, the results indicated that the affinity of the three compounds for CA proteins were PF-74 (Hexamer: $K_D = 0.12 \pm 0.00 \mu\text{M}$; Monomer: $K_D = 7.15 \pm 0.28 \mu\text{M}$) > **V-25i** (Hexamer: $K_D = 4.21 \pm 0.57 \mu\text{M}$; Monomer: $K_D = 11.62 \pm 1.63 \mu\text{M}$) > **II-13c** (Hexamer: $K_D = 4.82 \pm 0.30 \mu\text{M}$; Monomer: $K_D = 15.81 \pm 0.47 \mu\text{M}$), which is consistent with antiviral activity *in vitro* (PF-74, $EC_{50} = 0.42 \pm 0.11 \mu\text{M}$ > **V-25i**, $EC_{50} = 2.57 \pm 0.79 \mu\text{M}$ > **II-13d**, $EC_{50} = 5.14 \pm 1.62 \mu\text{M}$). SPR experiments demonstrated these compounds can be defined as HIV-1 CA protein inhibitors.

2.4. Molecular dynamics (MD) simulation

In order to understand the activity results and further explore the binding mode of these compounds with HIV-1 CA hexamer (PDB code: 5HGL, <https://www.rcsb.org>), **II-13c** and **V-25i** were chosen to make molecular dynamics (MD) simulation.

II-13c exhibited docking score, XP Gscore, and binding free energy values of -3.084 kcal/mol, -3.084 kcal/mol and -43.70 kcal/mol, respectively, and those for **V-25i** were -3.286 , -3.286 and -70.63 kcal/mol, respectively. It is shown that the affinity between **V** and **25i** and the action site of HIV-1 CA is higher than that of **II-13c**, which is consistent with the antiviral activity results at the cell level and the SPR results.

Compound **II-13c** interacted with the residues Asn53 and Asn57 of the capsid protein through H-bonds, and pi-cation (Lys70) as shown in Fig.3a. Likewise, compound **V-25i** interacted with the binding site residue Asn57 and Lys70 through H-bond and pi-cation, respectively (Fig.3b).

Next, as a part of the investigation, the binding and conformational stability of both complexes for **II-13c** and **V-25i** with CA was analyzed by MD simulation studies. As shown in Fig.4 and Fig.5, the binding conformation of **II-13c** and **V-25i** were stable in the binding pocket of capsid (PDB code: 5HGL) during the period of 50 ns MD simulation process. The protein structure stabilized nearly at 20 ns and the average root mean square deviation (RMSD) of C α was noted as 4.2 Å (Fig.4). The interaction of **II-13c** and **V-25i** with binding site residues through H-bond (green), hydrophobic interaction (grey), and water-bridge (blue) are presented in Fig.4 and Fig.5. The residues, Asn57 and Tyr130 interacted to **II-13c** by water bridges (Fig.4b, c). The residues Lys70 and Asn53 interacted to **II-13c** by pi-cation and H-bond, respectively (Fig.4b, c). Compound **II-13c** was always bounded with 6–7 contacts during the MD simulations (Fig.4d). The **V-25i**-capsid complex, protein structure stabilized in the early period of simulation with average C α -RMSD of 3.24 Å (Fig.5a). And **V-25i** exhibited interactions to the residues Asn53, Asn57, and Lys70 by water bridge interaction which facilitates the **V-25i** stability within the binding pocket (Fig.5b, c). The residue Lys70 also interacted to compound **V-25i** with pi-cation interactions. **V-25i** remained interacted with 7–8 contacts during the MD simulation process (Fig.5d). The Ramachandran mapping of the residues in the complex with **II-13c** and **V-25i** after MD simulation, supported a very acceptable number of residues in favored, additional allowed and generously allowed region (Table 3, entry 1 and 2). There were no residues present in outlier region of the capsid protein in complex with **V-25i** while 0.5% (Val181) residue observed outlier in **II-13c**-capsid complex (Fig. 6).

In conclusion, in silico study supported the experimental results for compounds **II-13c** and **V-25i** active against HIV-1. Compound **V-25i** showed better docking score, XP-Gscore and binding free energy with capsid protein over **II-13c**, which further validated by MD simulation for 50 ns that indicated high conformational stability for the former. This could be the reason variations in EC₅₀ of both compounds, however more biochemical assays are needed to be performed to validate.

3. Conclusion

In brief, taking the widely studied HIV-1 CA inhibitor PF-74 as the lead compound, we designed and synthesized 32 novel PF-74 derivatives via scaffold hopping. The antiviral activity of the compounds was significantly affected by the slight change of the linkers and substituents targeting CTD of CA protein. Among them, a lot of compounds of series **II** and **V** displayed moderate anti-HIV-1 activity in MT-4 cells. The most potent compounds in these two series are **II-13c** ($EC_{50} = 5.14 \pm 1.62 \mu\text{M}$, $CC_{50} > 9.51 \mu\text{M}$) and **V-25i** ($EC_{50} = 2.57 \pm 0.79 \mu\text{M}$, $CC_{50} > 8.55 \mu\text{M}$), though the activity was slightly weaker than PF-74 ($EC_{50} = 0.42 \pm 0.11 \mu\text{M}$, $CC_{50} > 11.56 \mu\text{M}$). Subsequently, the SPR assays indicated that these compounds are more inclined to combine with HIV-1 CA hexamer than monomer. Further molecular dynamics simulation exhibited that the binding conformation between **V** and **25i** and CA hexamer is more stable than **II-13c**, which is consistent with the results of antiviral activity in *vitro* and target affinity analysis.

In conclusion, this study enriched the SARs of PF-74 derivatives, and laid a solid foundation for finding novel and potent HIV-1 CA inhibitors.

4. Experimental section

4.1. Chemistry

^1H NMR and ^{13}C NMR spectra were recorded on a Bruker Avance-400 NMR spectrometer (Standard G1313A instrument) in DMSO. Chemical shifts were reported in δ values (ppm) and J values were presented in hertz (Hz). High resolution mass spectra (HRMS) were obtained from Thermo Electron LTQ-Orbitrap XL mass spectrometry instrument (Thermo Scientific Inc., USA). Melting points of all the compounds were measured on a micro melting point apparatus and were uncorrected. Flash column chromatography was performed on column packed with Silica Gel 60 (200–300 mesh). Solvents were reagent grade and purified with standard methods when necessary. Sample purity was analyzed on a Shimadzu SPD-20A/20AV high-performance liquid chromatography (HPLC) system with a Inertsil ODS-SP, 5 μm C18 column (150 \times 4.6 mm) [HPLC conditions: methanol/water (80/20); flow rate: 1.0 mL/min; UV detection from 210 to 400 nm; temperature: ambient; and injection volume: 20 μL]. Purity of all final compounds was $> 95\%$.

4.1.1. Synthesis of tert-butyl (S)-(1-((4-methoxyphenyl)(methyl)amino)-1-oxo-3-phenylpropan-2-yl)carbamate (6)—A solution of (*tert*-butoxycarbonyl)-L-phenylalanine (2.65 g, 10.00 mmol) in 15 mL dichloromethane was added PyBop (5.70 g, 15.00 mmol) at 0°C, and the mixture stirred for 0.5 h. Subsequently, DIEA (3.30 mL, 20.00 mmol) and 4-methoxy-*N*-methylaniline (1.37 g, 10.00 mmol) were added and then the mixture was stirred at room temperature for another 8 h (monitored by TLC), evaporated under reduced pressure and the residue was initially washed by saturated sodium bicarbonate (50 mL) and extracted with ethyl acetate (3 \times 10 mL). Then the combined organic layer was washed by 1 N HCl and extracted with ethyl acetate (3 \times 10 mL), dried over anhydrous Na_2SO_4 , filtered, and concentrated under reduced pressure to afford corresponding crude intermediate **6** as yellow oil with a yield of 79%. ^1H NMR (400 MHz, $\text{DMSO}-d_6$) δ 7.21 (d, $J = 8.4$ Hz, 3H, Ph-H + NH), 7.15 (d, $J = 7.1$ Hz, 2H, Ph-H), 7.02 (d, $J = 8.4$ Hz, 2H, Ph-H),

6.85–6.75 (m, 2H, Ph-H), 4.15 (q, $J = 5.4$ Hz, 1H, CH), 3.80 (s, 3H, OCH₃), 3.12 (s, 3H, NCH₃), 2.81–2.54 (m, 2H, CH₂), 1.30 (s, 9H, CH₃ × 3); ¹³C NMR (100 MHz, DMSO-*d*₆) δ 172.2, 158.9, 155.7, 138.5, 136.1, 129.2, 128.4, 126.7, 115.2, 78.3, 55.9, 53.5, 37.8, 37.1, 28.6. ESI-MS: m/z 385 [M + H]⁺, C₂₂H₂₈N₂O₄ (384.2).

4.1.2. Synthesis of (S)-2-amino-N-(4-methoxyphenyl)-N-methyl-3-phenylpropanamide (7)—Trifluoroacetic acid (2.36 mL, 31.56 mmol) was added dropwise to intermediate 6 (3.03 g, 7.89 mmol, 1.0 eq) in 30 mL dichloromethane and the resulting mixture solution was stirred at room temperature for 6–7 h. Then, the resulting solution was alkalinized to pH 9 with saturated sodium bicarbonate solution, and then extracted with dichloromethane (3 × 20 mL). The combined organic layer was dried over anhydrous Na₂SO₄, filtered, and concentrated under reduced pressure to yield the crude product 7 as yellow oil with a yield of 94%. ESI-MS: m/z 285 [M + H]⁺, C₁₇H₂₀N₂O₂ (284.1)

4.1.3. Synthetic route of methyl (S)-3-(N-(1-((4-methoxyphenyl)(methyl)amino)-1-oxo-3-phenylpropan-2-yl)sulfamoyl)benzoate (8)—Intermediate 7 (0.28 g, 1.00 mmol) was dissolved in 10 mL dichloromethane, and the mixture was added triethylamine (0.21 mL, 1.50 mmol). Subsequently, methyl 3-(chlorosulfonyl)benzoate (0.26 g, 1.10 mmol) was added to the mixture at 0 °C for another 4 h (monitored by TLC). Then the mixture was washed by saturated sodium bicarbonate (15 mL) and extracted with dichloromethane (3 × 8 mL). Then the mixture was dried over anhydrous Na₂SO₄, filtered, and concentrated under reduced pressure to afford product 8. White solid, yield: 60%. ¹H NMR (400 MHz, DMSO-*d*₆) δ 8.53 (d, $J = 9.0$ Hz, 1H, NH), 8.04 (d, $J = 7.7$ Hz, 1H, PhH), 7.95 (s, 1H, PhH), 7.67 (d, $J = 7.7$ Hz, 1H, PhH), 7.53 (t, $J = 7.7$ Hz, 1H, PhH), 7.12–6.96 (m, 7H, PhH), 6.64 (d, $J = 4.4$ Hz, 2H, PhH), 3.91 (s, 3H, OCH₃), 3.81 (s, 3H, OCH₃), 3.78 (dd, $J = 9.5, 3.6$ Hz, 1H, CH), 2.96 (s, 3H, NCH₃), 2.81 (dd, $J = 13.6, 3.6$ Hz, 1H, CH₂), 2.55 (s, 1H, CH₂). ESI-MS: m/z 483 [M + H]⁺, C₂₅H₂₆N₂O₆S (482.15).

4.1.4. Synthetic route of (S)-3-(N-(1-((4-methoxyphenyl)(methyl)amino)-1-oxo-3-phenylpropan-2-yl)sulfamoyl)benzoic acid (9)—8 was dissolved in 5 mL tetrahydrofuran. Then aqueous NaOH solution (5 mL) was added to the mixture and stirred for another 2 h (monitored by TLC). Subsequently, the resulting mixture solution was alkalinized to pH 2 with 1 N HCl to produce white precipitate, filtered, dried to afford 9. White solid, yield: 78%. ESI-MS: 467 m/z [M – H][–], C₂₄H₂₄N₂O₆S (468.14).

4.1.5. General procedure for the synthesis of target compounds I-10(a–e)—A solution of 9 (1.0 eq) in 15 mL dichloromethane was added PyBop (1.5 eq) at 0 °C, and the mixture stirred for 0.5 h. Subsequently, DIEA (2.0 eq) and amine fragments (2.0 eq) were added to the mixture and then stirred at room temperature for another 8 h (monitored by TLC). The resulting mixture was evaporated under reduced pressure and the residue was initially washed by saturated sodium bicarbonate (15 mL) and extracted with dichloromethane (3 × 8 mL). Then the combined organic layer was washed by 1 N HCl and extracted with dichloromethane (3 × 8 mL), dried over anhydrous Na₂SO₄, filtered, and concentrated under reduced pressure to afford product I-10 (a–e). Yield: 40–70%.

(S)-N-cyclopropyl-3-(N-(1-((4-methoxyphenyl)(methyl)amino)-1-oxo-3-phenylpropan-2-yl)sulfamoyl)benzamide (I-10a): white solid, yield: 61%, HPLC purity 98% (t_R = 4.02 min), mp: 175–177°C. ^1H NMR (400 MHz, DMSO- d_6) δ 8.65 (d, J = 3.7 Hz, 1H, NH), 8.38 (d, J = 9.0 Hz, 1H, PhH), 8.03 (s, 1H, NH), 7.95 (d, J = 7.5 Hz, 1H, PhH), 7.54 (d, J = 7.7 Hz, 1H, PhH), 7.47 (t, J = 7.7 Hz, 1H, PhH), 7.10 (d, J = 4.8 Hz, 3H, PhH), 7.03 – 6.90 (m, 4H, PhH), 6.71 (d, J = 4.5 Hz, 2H, PhH), 3.80 (s, 4H, CH + OCH₃), 2.96 (s, 1H, CH), 2.93 (s, 3H, NCH₃), 2.87 – 2.77 (m, 2H, CH₂), 0.74 (d, J = 5.6 Hz, 2H, CH₂), 0.64 – 0.58 (m, 2H, CH₂). ^{13}C NMR (100 MHz, DMSO- d_6) δ 170.4, 166.5, 159.1, 141.3, 137.2, 135.4, 135.2, 130.9, 129.3, 129.2, 129.0, 128.4, 126.9, 125.9, 115.1, 55.9, 54.8, 38.3, 37.5, 23.6, 6.1. HRMS (ESI) calcd for C₂₇H₂₉N₃O₅S [M + H]⁺ 508.1828, found 508.1894.

(S)-N-(4-methoxyphenyl)-N-methyl-2-((3-(morpholine-4-carbonyl) phenyl)sulfonamido)-3-phenylpropanamide (I-10b) : white solid, yield: 57%, HPLC purity 99% (t_R = 3.76 min), mp: 141–143°C. ^1H NMR (400 MHz, DMSO- d_6) δ 8.45 (d, J = 8.9 Hz, 1H, NH), 7.53 (td, J = 17.6, 15.1, 7.4 Hz, 4H, PhH), 7.11 (s, 3H, PhH), 6.95 (d, J = 8.0 Hz, 4H, PhH), 6.80 – 6.69 (m, 2H, PhH), 3.79 (s, 4H, CH + OCH₃), 3.68 (d, J = 19.6 Hz, 4H, CH₂ × 2), 3.56 (d, J = 8.0 Hz, 2H, CH₂), 3.23 (s, 2H, CH₂), 2.92 (s, 3H, NCH₃), 2.88 – 2.79 (m, 1H, CH₂), 2.62 – 2.54 (m, 1H, CH₂). ^{13}C NMR (100 MHz, DMSO- d_6) δ 170.4, 168.0, 159.1, 141.6, 137.2, 136.3, 135.4, 130.9, 129.5, 129.3, 129.0, 128.5, 127.7, 126.9, 125.4, 115.1, 66.4, 55.9, 54.8, 38.7, 38.3, 37.5. HRMS (ESI) calcd for C₂₈H₃₁N₃O₆S [M + H]⁺ 538.1934, found 538.2010.

(S)-2-((3-(2,3-dihydro-1H-pyrrolo[3,4-c]pyridine-2-carbonyl)phenyl) sulfonamido)-N-(4-methoxyphenyl)-N-methyl-3-phenylpropanamide (I-10c): white solid, yield: 52%, HPLC purity 97% (t_R = 4.37 min), mp: 80–82 °C. ^1H NMR (400 MHz, DMSO- d_6) δ 8.39 (d, J = 8.9 Hz, 1H, pyridinyl-H), 7.66 (dd, J = 13.2, 5.2 Hz, 4H, NH + PhH × 3), 7.57 (d, J = 7.8 Hz, 1H, PhH), 7.46 (t, J = 7.9 Hz, 1H, PhH), 7.14 (s, 3H, PhH), 6.96 – 6.81 (m, 4H, PhH × 2 + pyridinyl-H × 2), 6.82 – 6.70 (m, 4H, PhH), 4.16 (t, J = 8.1 Hz, 2H, CH₂), 3.89 – 3.80 (m, 1H, CH), 3.75 (s, 3H, OCH₃), 3.16 (t, J = 8.0 Hz, 2H, CH₂), 2.93 (s, 3H, NCH₃), 2.86 (dd, J = 13.4, 5.4 Hz, 1H, CH₂), 2.60 – 2.54 (m, 1H, CH₂). ^{13}C NMR (100 MHz, DMSO- d_6) δ 170.4, 167.0, 159.0, 155.6, 145.7, 140.8, 137.3, 137.1, 135.3, 134.3, 132.3, 129.4, 128.9, 128.5, 126.9, 126.7, 126.5, 119.2, 115.0, 55.8, 54.6, 47.7, 38.7, 37.5, 24.7. HRMS (ESI) calcd for C₃₁H₃₀N₄O₅S [M + H]⁺ 571.1937, found 571.2009.

(S)-N-(4-methoxyphenyl)-3-(N-(1-((4-methoxyphenyl)(methyl) amino)-1-oxo-3-phenylpropan-2-yl)sulfamoyl)-N-methylbenzamide (I-10d): brown solid, yield: 47%, HPLC purity 98% (t_R = 4.84 min), mp: 60–62 °C. ^1H NMR (400 MHz, DMSO- d_6) δ 8.31 (d, J = 9.0 Hz, 1H, NH), 7.65 (s, 1H, PhH), 7.28 (d, J = 8.0 Hz, 3H, PhH), 7.10 (qd, J = 7.9, 7.4, 4.3 Hz, 5H, PhH), 6.95 (d, J = 8.1 Hz, 2H, PhH), 6.87 (d, J = 8.4 Hz, 2H, PhH), 6.77 (d, J = 8.5 Hz, 2H, PhH), 6.72 (d, J = 6.8 Hz, 2H, PhH), 3.79 (s, 3H, OCH₃), 3.77 – 3.72 (m, 1H, CH), 3.64 (s, 3H, OCH₃), 3.35 (s, 3H, NCH₃), 2.94 (s, 3H, NCH₃), 2.82 (dd, J = 13.6, 5.4 Hz, 1H, CH₂), 2.49 – 2.40 (m, 1H, CH₂). ^{13}C NMR (100 MHz, DMSO- d_6) δ 170.4, 159.0, 158.1, 141.1, 137.3, 137.1, 135.4, 131.7, 129.3, 129.0, 128.7, 128.5, 127.3, 126.9, 115.1, 114.8, 55.9, 55.6, 54.6, 38.4, 37.6. HRMS (ESI) calcd for C₃₂H₃₃N₃O₆S [M + H]⁺ 589.2169, found 588.2169.

(S)-*N*-(benzo[*d*]thiazol-6-yl)-3-(*N*-(1-((4-methoxyphenyl)(methyl) amino)-1-oxo-3-phenylpropan-2-yl)sulfamoyl)benzamide (**I-10e**): white solid, yield: 73%, HPLC purity 98% ($t_R = 4.81$ min) purity: 98%, mp: 190–192 °C. ^1H NMR (400 MHz, DMSO- d_6) δ 10.70 (s, 1H, NH), 9.33 (s, 1H, thiazyl-H), 8.71 (s, 1H, NH), 8.47 (d, $J = 8.9$ Hz, 1H, PhH), 8.16 (s, 1H, PhH), 8.13 – 8.05 (m, 2H, PhH), 7.86 (d, $J = 8.8$ Hz, 1H, PhH), 7.65 (d, $J = 7.7$ Hz, 1H, PhH), 7.58 (t, $J = 7.7$ Hz, 1H, PhH), 7.07 (s, 3H, PhH), 7.01 (d, $J = 7.8$ Hz, 2H, PhH), 6.95 (d, $J = 8.2$ Hz, 2H, PhH), 6.76 – 6.67 (m, 2H, PhH), 3.82 (t, $J = 10.8$ Hz, 1H, CH), 3.74 (s, 3H, OCH₃), 2.96 (s, 3H, NCH₃), 2.83 (dd, $J = 13.5, 3.7$ Hz, 1H, CH₂), 2.61 – 2.54 (m, 1H, CH₂). ^{13}C NMR (100 MHz, DMSO- d_6) δ 170.5, 164.8, 159.1, 155.6, 150.1, 141.5, 137.2, 137.0, 135.5, 135.4, 134.6, 131.5, 129.7, 129.4, 129.2, 129.0, 128.4, 126.8, 126.4, 123.3, 120.4, 115.2, 113.6, 55.8, 54.9, 38.2, 37.6. HRMS (ESI) calcd for C₃₁H₂₈N₄O₅S₂ [M + H]⁺ 601.1501, found 601.1573.

4.1.6. Synthetic route of methyl (S)-2-(N-(1-((4-methoxyphenyl)(methyl) amino)-1-oxo-3-phenylpropan-2-yl)sulfamoyl)acetate (11)—Intermediate **7** (0.28 g, 1.00 mmol) was dissolved in 15 mL dichloromethane, and the mixture was added triethylamine (0.21 mL, 1.50 mmol). Subsequently, methyl 2-(chlorosulfonyl)acetate (0.12 mL, 1.00 mmol) was added to the mixture at 0°C for 4 h (monitored by TLC). Then the mixture was washed by saturated sodium bicarbonate (15 mL) and extracted with dichloromethane (3 × 8 mL). Then the mixture was dried over anhydrous Na₂SO₄, filtered, and concentrated under reduced pressure to afford product **11**. White solid, yield: 76%. ^1H NMR (400 MHz, DMSO- d_6) δ 8.06 (d, $J = 8.6$ Hz, 1H, NH), 7.22 (d, $J = 6.2$ Hz, 3H, PhH), 7.04 (s, 2H, PhH), 6.99 (d, $J = 8.2$ Hz, 2H, PhH), 6.86 (d, $J = 6.8$ Hz, 2H, PhH), 4.08 (td, $J = 8.8, 4.9$ Hz, 1H, CH), 3.87 – 3.77 (m, 4H, OCH₃ + CH₂), 3.69 (d, $J = 14.7$ Hz, 1H, CH₂), 3.60 (s, 3H, OCH₃), 3.13 (s, 3H, NCH₃), 2.87 (dd, $J = 13.4, 4.9$ Hz, 1H, CH₂), 2.66 (dd, $J = 13.1, 9.5$ Hz, 1H, CH₂). ESI-MS: m/z 421 [M + H]⁺, 443 [M + Na]⁺, C₂₀H₂₄N₂O₆S (500.15).

4.1.7. Synthetic route of (S)-2-(N-(1-((4-methoxyphenyl)(methyl)amino)-1-oxo-3-phenylpropan-2-yl)sulfamoyl)acetic acid (12)—**11** was dissolved in 5 mL tetrahydrofuran. Then aqueous solution containing NaOH (5 mL) was added to the mixture and stirred for another 2 h (monitored by TLC). Subsequently, the resulting mixture solution was alkalinized to pH 2 with 1 N HCl to produce white precipitate, which was filtered, dried to afford **12**. White solid, yield: 89%. ESI-MS: m/z 405 [M – H][–], C₁₉H₂₂N₂O₆S (406.12).

4.1.8. General procedure for the synthesis of target compounds II-13(a–g)—A solution of **12** (1.0 eq) in 15 mL dichloromethane was added PyBop (1.5 eq) at room temperature, and the mixture stirred for 0.5 h. Subsequently, DIEA (2.0 eq) and amine fragments (2.0 eq) were added to the mixture and then stirred at room temperature for another 8 h (monitored by TLC). The resulting mixture was initially washed by saturated sodium bicarbonate (15 mL) and extracted with dichloromethane (3 × 8 mL). Then the combined organic layer was washed by 1 N HCl and extracted with dichloromethane (3 × 8 mL). Then the combined organic phase was washed with saturated salt water (3 × 10 mL), dried over anhydrous Na₂SO₄, filtered, and recrystallized with ethyl acetate and petroleum ether to afford product **II-13(a–g)**. Yield: 40–70%.

(S)-2-((2-((4-cyanophenyl)amino)-2-oxoethyl)sulfonamido)-*N*-(4-methoxyphenyl)-*N*-methyl-3-phenylpropanamide (**II-13a**): yellow solid, yield: 56%, HPLC purity 97% ($t_R = 4.30$ min), mp: 82–84 °C. ^1H NMR (400 MHz, DMSO- d_6) δ 10.70 (s, 1H, NH), 8.13 (d, $J = 8.4$ Hz, 1H, NH), 7.83 (d, $J = 8.1$ Hz, 2H, PhH), 7.77 (d, $J = 8.3$ Hz, 2H, PhH), 7.21 (d, $J = 5.4$ Hz, 3H, PhH), 7.03 (s, 2H, PhH), 6.93 (d, $J = 8.3$ Hz, 2H, PhH), 6.85 (d, $J = 6.5$ Hz, 2H, PhH), 4.16 (q, $J = 8.0$ Hz, 1H, CH), 3.90 (s, 2H, CH₂), 3.78 (s, 3H, OCH₃), 3.13 (s, 3H, NCH₃), 2.89 (dd, $J = 13.2, 5.3$ Hz, 1H, CH₂), 2.73 (d, $J = 9.5$ Hz, 1H, CH₂). ^{13}C NMR (100 MHz, DMSO- d_6) δ 171.4, 161.4, 159.1, 143.1, 137.3, 135.4, 133.7, 129.5, 129.1, 128.6, 127.1, 119.8, 119.4, 115.1, 106.0, 60.6, 55.9, 55.6, 38.7, 38.2. HRMS (ESI) calcd for C₂₆H₂₆N₄O₅S [M + H]⁺ 507.1624, found 507.1689. *(S)*-2-((2-(benzo[d]thiazol-6-ylamino)-2-oxoethyl)sulfonamido)-*N*-(4-methoxyphenyl)-*N*-methyl-3-phenylpropanamide (**II-13b**): white solid, yield: 57%, HPLC purity 97% ($t_R = 4.18$ min), mp: 110–112 °C. ^1H NMR (400 MHz, DMSO- d_6) δ 10.55 (s, 1H, NH), 9.31 (s, 1H, thiazyl-H), 8.51 (s, 1H, NH), 8.06 (d, $J = 8.5$ Hz, 2H, PhH), 7.61 (d, $J = 8.8$ Hz, 1H, PhH), 7.20 (d, $J = 4.0$ Hz, 3H, PhH), 7.02 (s, 2H, PhH), 6.88 (dd, $J = 17.9, 6.8$ Hz, 4H, PhH), 4.19 (q, $J = 7.9$ Hz, 1H, CH), 3.91 (s, 2H, CH₂), 3.74 (s, 3H, OCH₃), 3.13 (s, 3H, NCH₃), 2.90 (dd, $J = 13.7, 5.7$ Hz, 1H, CH₂), 2.80 – 2.72 (m, 1H, CH₂). ^{13}C NMR (100 MHz, DMSO- d_6) δ 171.4, 160.8, 159.0, 155.5, 149.9, 137.3, 136.7, 135.4, 134.7, 129.6, 129.1, 128.6, 127.0, 123.5, 119.3, 115.1, 112.3, 60.6, 55.8, 55.6, 38.6, 38.1. HRMS (ESI) calcd for C₂₆H₂₆N₄O₅S₂ [M + H]⁺ 539.1345, found 539.1415.

(S)-*N*-(4-methoxyphenyl)-2-((2-((4-methoxyphenyl)(methyl)amino)-2-oxoethyl)sulfonamido)-*N*-methyl-3-phenylpropanamide (**II-13c**): white solid, yield: 61%, HPLC purity 98% ($t_R = 6.97$ min), mp: 100–102 °C. ^1H NMR (400 MHz, DMSO- d_6) δ 7.93 (d, $J = 4.8$ Hz, 1H, NH), 7.67 (d, $J = 8.4$ Hz, 2H, PhH), 7.15 (p, $J = 6.7$ Hz, 3H, PhH), 7.11 – 6.94 (m, 4H, PhH), 6.92 (d, $J = 9.0$ Hz, 2H, PhH), 6.85 (d, $J = 6.6$ Hz, 2H, PhH), 4.88 (d, $J = 14.4$ Hz, 1H, CH₂), 4.73 (d, $J = 14.4$ Hz, 1H, CH₂), 4.16 (td, $J = 8.9, 5.3$ Hz, 1H, CH), 3.94 (s, 3H, OCH₃), 3.78 (s, 3H, OCH₃), 3.05 (s, 6H, NCH₃ × 2), 2.83 (dd, $J = 13.4, 5.2$ Hz, 1H, CH₂), 2.65 (dd, $J = 13.5, 8.9$ Hz, 1H, CH₂). ^{13}C NMR (150 MHz, DMSO- d_6) δ 171.1, 161.0, 159.0, 155.0, 145.8, 137.5, 135.6, 134.7, 129.6, 129.1, 128.5, 127.0, 126.9, 119.1, 115.1, 57.9, 55.9, 55.4, 46.1, 38.7, 37.9, 23.8. HRMS (ESI) calcd for C₂₇H₃₁N₃O₆S [M + H]⁺ 526.1934, found 526.2011.

(S)-2-((2-(5-methoxyindolin-1-yl)-2-oxoethyl)sulfonamido)-*N*-(4-methoxyphenyl)-*N*-methyl-3-phenylpropanamide (**II-13d**): brown solid, yield: 57%, HPLC purity 99% ($t_R = 5.09$ min), mp: 98–100 °C. ^1H NMR (400 MHz, DMSO- d_6) δ 7.94 (d, $J = 8.2$ Hz, 2H, PhH + NH), 7.21 (s, 3H, PhH), 7.03 (s, 2H, PhH), 6.93 (d, $J = 8.1$ Hz, 2H, PhH), 6.86 (s, 3H, PhH), 6.73 (d, $J = 8.7$ Hz, 1H, PhH), 4.14 (d, $J = 6.6$ Hz, 1H, CH), 4.02 (t, $J = 8.5$ Hz, 2H, CH₂), 3.91 (d, $J = 14.2$ Hz, 1H, CH₂), 3.79 (d, $J = 10.4$ Hz, 4H, OCH₃ + CH₂), 3.72 (s, 3H, OCH₃), 3.09 (d, $J = 12.4$ Hz, 5H, NCH₃ + CH₂), 2.87 (dd, $J = 13.4, 5.4$ Hz, 1H, CH₂), 2.73 – 2.66 (m, 1H, CH₂). ^{13}C NMR (100 MHz, DMSO- d_6) δ 170.9, 159.7, 159.0, 156.6, 137.5, 136.3, 135.5, 134.3, 129.6, 129.2, 128.7, 127.1, 117.4, 115.1, 112.2, 111.2, 59.2, 55.9, 55.8, 55.6, 48.7, 38.7, 37.9, 27.8. HRMS (ESI) calcd for C₂₈H₃₁N₃O₆S [M + H]⁺ 538.1934, found 538.2016.

(S)-2-((2-((3,5-difluorophenyl)amino)-2-oxoethyl)sulfonamido)-*N*-(4-methoxyphenyl)-*N*-methyl-3-phenylpropanamide (**II-13e**): white solid, yield: 67%, HPLC purity 98% ($t_R = 6.03$ min), mp: 156–158 °C. ^1H NMR (400 MHz, DMSO- d_6) δ 10.65 (s, 1H, NH), 8.13 (d, $J = 8.3$ Hz, 1H, NH), 7.28 (d, $J = 8.7$ Hz, 2H, PhH), 7.19 (s, 3H, PhH), 7.00 (dd, $J = 19.9, 9.0$ Hz, 3H, PhH), 6.93 (d, $J = 8.3$ Hz, 2H, PhH), 6.84 (d, $J = 6.3$ Hz, 2H, PhH), 4.15 (q, $J = 7.9$ Hz, 1H, CH), 3.85 (d, $J = 4.7$ Hz, 2H, CH₂), 3.77 (s, 3H, OCH₃), 3.12 (s, 3H, NCH₃), 2.88 (dd, $J = 13.5, 5.3$ Hz, 1H, CH₂), 2.70 (dd, $J = 13.7, 8.8$ Hz, 1H, CH₂). ^{13}C NMR (100 MHz, DMSO- d_6) δ 171.4, 162.8 (dd, $^1J_{\text{CF}} = 243.4, ^3J_{\text{CF}} = 15.2$ Hz), 161.3, 159.0, 141.4 (t, $^3J_{\text{CF}} = 13.7$ Hz), 137.4, 135.4, 129.5, 129.1, 128.6, 127.1, 115.1, 102.7 (d, $^2J_{\text{CF}} = 29.4$ Hz), 99.4 (t, $^2J_{\text{CF}} = 26.2$ Hz), 60.6, 55.8, 55.6, 38.5, 38.1. HRMS (ESI) calcd for C₂₅H₂₅F₂N₃O₅S [M + H]⁺ 518.1483, found 518.1561.

(S)-2-((2-(1*H*-indazol-1-yl)-2-oxoethyl)sulfonamido)-*N*-(4-methoxyphenyl)-*N*-methyl-3-phenylpropanamide (**II-13f**): white solid, yield: 64%, HPLC purity 99% ($t_R = 3.76$ min), mp: 68–70 °C. ^1H NMR (400 MHz, DMSO- d_6) δ 8.53 (s, 1H, pyrazoly-H), 8.29 (d, $J = 8.3$ Hz, 1H, NH), 8.25 (d, $J = 8.7$ Hz, 1H, PhH), 7.95 (d, $J = 7.9$ Hz, 1H, PhH), 7.68 (t, $J = 7.7$ Hz, 1H, PhH), 7.48 (t, $J = 7.5$ Hz, 1H, PhH), 7.13 (dt, $J = 13.1, 6.4$ Hz, 5H, PhH), 6.98 (d, $J = 8.2$ Hz, 2H, PhH), 6.82 (d, $J = 7.3$ Hz, 2H, PhH), 4.84 (d, $J = 14.3$ Hz, 1H, CH₂), 4.66 (d, $J = 14.7$ Hz, 1H, CH₂), 4.17 (td, $J = 9.1, 4.8$ Hz, 1H, CH), 3.80 (s, 3H, OCH₃), 3.10 (s, 3H, NCH₃), 2.86 (dd, $J = 13.8, 4.9$ Hz, 1H, CH₂), 2.70–2.63 (m, 1H, CH₂). ^{13}C NMR (100 MHz, DMSO- d_6) δ 171.0, 162.9, 159.1, 141.6, 138.6, 137.4, 135.6, 130.4, 129.5, 128.5, 126.9, 125.7, 122.4, 115.2, 115.1, 57.4, 55.9, 55.7, 38.3, 38.0. HRMS (ESI) calcd for C₂₆H₂₆N₄O₅S [M + H]⁺ 507.1624, found 507.1701.

(S)-*N*-(4-methoxyphenyl)-*N*-methyl-2-((2-(5-nitroindolin-1-yl)-2-oxoethyl)sulfonamido)-3-phenylpropanamide (**II-13g**): brown solid, yield: 57%, HPLC purity 99% ($t_R = 5.17$ min), mp: 92–94 °C. ^1H NMR (400 MHz, DMSO- d_6) δ 8.14 (s, 3H, NH + PhH \times 2), 8.06 (d, $J = 8.4$ Hz, 1H, PhH), 7.20 (d, $J = 6.4$ Hz, 3H, PhH), 7.02 (s, 2H, PhH), 6.93 (d, $J = 8.2$ Hz, 2H, PhH), 6.86 (d, $J = 6.8$ Hz, 2H, PhH), 4.16 (q, $J = 7.4, 6.2$ Hz, 3H, CH + CH₂), 4.07 (d, $J = 14.5$ Hz, 1H, CH₂), 3.93 (d, $J = 14.4$ Hz, 1H, CH₂), 3.77 (s, 3H, OCH₃), 3.25 (t, $J = 8.7$ Hz, 2H, CH₂), 3.07 (s, 3H, NCH₃), 2.87 (dd, $J = 13.5, 5.4$ Hz, 1H, CH₂), 2.70 (d, $J = 11.5$ Hz, 1H, CH₂). ^{13}C NMR (100 MHz, DMSO- d_6) δ 170.9, 162.2, 159.0, 148.4, 143.7, 137.4, 135.5, 134.8, 129.6, 129.2, 128.7, 127.1, 124.6, 120.9, 116.1, 115.1, 59.4, 55.9, 55.7, 49.5, 38.6, 37.9, 27.1. HRMS (ESI) calcd for C₂₇H₂₈N₄O₇S [M + H]⁺ 553.1679, found 553.1754.

4.1.9. Synthetic route of methyl (*S*)-2-((1-((4-methoxyphenyl)(methyl)amino)-1-oxo-3-phenylpropan-2-yl)amino)-2-oxoacetate (**14**)—Intermediate **7**

(0.28 g, 1.00 mmol) was dissolved in 15 mL dichloromethane, and the mixture was added triethylamine (0.21 mL, 1.50 mmol). Subsequently, methyl 2-chloro-2-oxoacetate (0.21 mL, 1.50 mmol) was added slowly to the mixture at 0 °C for another 4 h (monitored by TLC). Then the mixture was washed by saturated sodium bicarbonate (15 mL) and extracted with dichloromethane (3 \times 8 mL). Then the combined organic phase was washed with saturated salt water (3 \times 10 mL) and was dried over anhydrous Na₂SO₄, filtered, and recrystallized with ethyl acetate and petroleum ether to afford product **14**. White solid, yield: 73%. ^1H NMR (400 MHz, DMSO- d_6) δ 9.01 (d, $J = 7.8$ Hz, 1H, NH), 7.16 (t, $J = 9.5$ Hz, 5H, PhH), 7.00 (d, $J = 8.3$ Hz, 2H, PhH), 6.85 (d, $J = 6.9$ Hz, 2H, PhH), 4.48 (q, $J = 8.1$ Hz, 1H, CH),

3.80 (s, 3H, OCH₃), 3.74 (s, 3H, OCH₃), 3.12 (s, 3H, NCH₃), 2.88 (dt, *J* = 13.7, 7.2 Hz, 2H, CH₂). ESI-MS: *m/z* 371 [M + H]⁺, 393 [M + Na]⁺, C₂₀H₂₂N₂O₅ (370.15).

4.1.10. Synthetic route of (S)-2-((1-((4-methoxyphenyl)(methyl)amino)-1-

oxo-3-Phenylpropan-2-yl)amino)-2-oxoacetic acid (15)—14 (0.10 g, 0.27 mmol) was dissolved in 5 mL tetrahydrofuran. Then aqueous solution containing NaOH (0.02 g, 0.54 mmol) was added to the mixture and stirred for 2 h (monitored by TLC). Subsequently, the resulting mixture solution was alkalized to pH 2 with 1 N HCl to produce white precipitate, filtered, dried to afford **15**. White solid, yield: 68%. ESI-MS: *m/z* 355 [M – H][–], C₁₉H₂₀N₂O₅ (356.14).

4.1.11. General procedure for the synthesis of target compounds III-16 (a–g)

—A solution of **15** (1.0 eq) in 15 mL dichloromethane was added PyBop (1.5 eq) at room temperature, and the mixture stirred for 0.5 h. Subsequently, DIEA (2.0 eq) and amine fragments (2.0 eq) were added to the mixture and then the resulting mixture was stirred at room temperature for another 8 h (monitored by TLC). The mixture was initially washed by saturated sodium bicarbonate (15 mL) and extracted with dichloromethane (3 × 8 mL). Then the combined organic layer was washed by 1 N HCl and extracted with dichloromethane (3 × 8 mL). Then the combined organic phase was washed with saturated salt water (3 × 10 mL), dried over anhydrous Na₂SO₄, filtered, and recrystallized with ethyl acetate and petroleum ether to afford product **III-16(a–g)**. Yield: 40–80%.

(S)-N1-(benzo[d]thiazol-6-yl)-N2-(1-((4-methoxyphenyl)(methyl) amino)-1-oxo-3-phenylpropan-2-yl)oxalamide (**III-16a**): white solid, yield: 53%, HPLC purity 99% (*t_R* = 5.81 min), mp: 78–80 °C. ¹H NMR (400 MHz, DMSO-*d*₆) δ 10.88 (s, 1H, NH), 9.32 (s, 1H, thiazyl-H), 8.90 (d, *J* = 7.9 Hz, 1H, NH), 8.63 (s, 1H, PhH), 8.04 (d, *J* = 8.8 Hz, 1H, PhH), 7.89 (d, *J* = 8.9 Hz, 1H, PhH), 7.26 (s, 2H, PhH), 7.18 (d, *J* = 7.2 Hz, 3H, PhH), 7.02 (d, *J* = 8.3 Hz, 2H, PhH), 6.90 (d, *J* = 7.0 Hz, 2H, PhH), 4.58 (q, *J* = 7.8 Hz, 1H, CH), 3.81 (s, 3H, OCH₃), 3.15 (s, 3H, NCH₃), 3.02 – 2.89 (m, 2H, CH₂). ¹³C NMR (100 MHz, DMSO-*d*₆) δ 170.6, 159.9, 159.2, 158.5, 156.0, 150.4, 137.8, 135.8, 135.7, 134.4, 129.3, 129.3, 127.0, 123.4, 120.3, 115.2, 113.6, 55.9, 52.6, 37.9, 36.8. HRMS (ESI) calcd for C₂₆H₂₄N₄O₄S [M + H]⁺ 489.1518, found 489.1592.

(S)-2-(2-(5-methoxyindolin-1-yl)-2-oxoacetamido)-N-(4-methoxyphenyl)-N-methyl-3-phenylpropanamide (**III-16b**): white solid, yield: 50%, HPLC purity 99% (*t_R* = 6.52 min), mp: 82–84 °C. ¹H NMR (400 MHz, DMSO-*d*₆) δ 9.00 (d, *J* = 7.8 Hz, 1H, NH), 7.90 (d, *J* = 8.8 Hz, 1H, PhH), 7.21 (dt, *J* = 16.2, 8.4 Hz, 5H, PhH), 7.04 (d, *J* = 8.1 Hz, 2H, PhH), 6.91 – 6.82 (m, 3H, PhH), 6.76 (d, *J* = 8.8 Hz, 1H, PhH), 4.63 – 4.50 (m, 1H, CH), 3.89 (q, *J* = 9.4 Hz, 1H, CH₂), 3.82 (s, 3H, OCH₃), 3.73 (s, 3H, OCH₃), 3.59 (q, *J* = 10.1, 9.6 Hz, 1H, CH₂), 3.15 (s, 3H, NCH₃), 3.00 (d, *J* = 8.2 Hz, 2H, CH₂), 2.93 (dd, *J* = 13.6, 4.2 Hz, 1H, CH₂), 2.75 (dd, *J* = 13.7, 9.9 Hz, 1H, CH₂). ¹³C NMR (100 MHz, DMSO-*d*₆) δ 170.7, 162.8, 160.7, 159.1, 157.0, 137.8, 135.9, 135.7, 134.7, 129.4, 129.2, 128.6, 126.9, 117.6, 115.3, 112.4, 111.3, 55.9, 55.8, 51.6, 48.6, 37.9, 37.2, 28.3. HRMS (ESI) calcd for C₂₈H₂₉N₃O₅ [M + H]⁺ 488.2107, found 488.2186.

(S)-N1-(4-methoxyphenyl)-N2-(1-((4-methoxyphenyl)(methyl) amino)-1-oxo-3-phenylpropan-2-yl)-N1-methyl oxalamide (III-16c): yellow solid, yield: 59%, HPLC purity 98% ($t_R = 4.02$ min), mp: 141–143 °C. $^1\text{H NMR}$ (400 MHz, DMSO- d_6) δ 8.88 (d, $J = 8.5$ Hz, 1H, NH), 7.20 (p, $J = 8.3, 7.8$ Hz, 5H, PhH), 7.06 (d, $J = 8.4$ Hz, 2H, PhH), 6.82 (t, $J = 6.9$ Hz, 3H, PhH), 6.70 (t, $J = 9.1$ Hz, 3H, PhH), 4.24 (q, $J = 7.6$ Hz, 1H, CH), 3.74 (s, 3H, OCH₃), 3.68 (s, 3H, OCH₃), 3.13 (s, 3H, NCH₃), 3.01 (s, 3H, NCH₃), 2.77 (dd, $J = 13.2, 6.5$ Hz, 1H, CH₂), 2.53 (s, 1H, CH₂). $^{13}\text{C NMR}$ (100 MHz, DMSO- d_6) δ 170.4, 164.9, 163.3, 158.8, 158.4, 137.6, 135.6, 135.1, 129.3, 128.8, 128.6, 127.9, 127.1, 126.9, 114.9, 114.4, 55.7, 55.7, 50.8, 37.8, 37.7, 36.3. HRMS (ESI) calcd for C₂₇H₂₉N₃O₅ [M + H]⁺ 476.2107, found 476.2185.

(S)-N1-(3,5-difluorophenyl)-N2-(1-((4-methoxyphenyl)(methyl) amino)-1-oxo-3-phenylpropan-2-yl)oxalamide (III-16d): white solid, yield: 74%, HPLC purity 99% ($t_R = 8.42$ min), mp: 132–134 °C. $^1\text{H NMR}$ (400 MHz, DMSO- d_6) δ 11.01 (s, 1H, NH), 8.99 (d, $J = 7.8$ Hz, 1H, NH), 7.58 (d, $J = 9.0$ Hz, 2H, PhH), 7.21 (dd, $J = 24.0, 7.3$ Hz, 5H, PhH), 7.02 (d, $J = 7.8$ Hz, 3H, PhH), 6.89 (d, $J = 7.0$ Hz, 2H, PhH), 4.55 (q, $J = 7.9$ Hz, 1H, CH), 3.81 (s, 3H, OCH₃), 3.15 (s, 3H, NCH₃), 3.06 – 2.88 (m, 2H, CH₂). $^{13}\text{C NMR}$ (100 MHz, DMSO- d_6) δ 170.5, 162.7 (dd, $^1J_{\text{CF}} = 243.0, ^3J_{\text{CF}} = 15.2$ Hz), 159.4, 159.2, 158.9, 140.5 (t, $^3J_{\text{CF}} = 14.0$ Hz), 137.8, 135.8, 129.2, 128.6, 127.0, 115.2, 103.8 (d, $^2J_{\text{CF}} = 29.7$ Hz), 100.2 (t, $^2J_{\text{CF}} = 26.6$ Hz), 55.9, 52.7, 37.9, 36.7. HRMS (ESI) calcd for C₂₅H₂₃F₂N₃O₄ [M + H]⁺ 468.1798, found 468.1730.

(S)-N1-(4-cyanophenyl)-N2-(1-((4-methoxyphenyl)(methyl) amino)-1-oxo-3-phenylpropan-2-yl)oxalamide (III-16e): white solid, yield: 62%, HPLC purity 98% ($t_R = 5.55$ min), mp: 117–119 °C. $^1\text{H NMR}$ (400 MHz, DMSO- d_6) δ 11.03 (s, 1H, NH), 9.00 (d, $J = 7.9$ Hz, 1H, NH), 7.99 (d, $J = 8.1$ Hz, 2H, PhH), 7.82 (d, $J = 8.0$ Hz, 2H, PhH), 7.24 (d, $J = 7.5$ Hz, 2H, PhH), 7.17 (q, $J = 6.9, 6.3$ Hz, 3H, PhH), 7.01 (d, $J = 8.2$ Hz, 2H, PhH), 6.88 (d, $J = 7.0$ Hz, 2H, PhH), 4.55 (q, $J = 7.6, 7.1$ Hz, 1H, CH), 3.80 (s, 3H, OCH₃), 3.14 (s, 3H, NCH₃), 2.96 (h, $J = 8.8$ Hz, 2H, CH₂). $^{13}\text{C NMR}$ (100 MHz, DMSO- d_6) δ 170.5, 159.5, 159.2, 159.0, 142.2, 137.8, 135.8, 133.6, 129.3, 128.6, 127.0, 120.9, 119.3, 115.2, 106.9, 55.9, 52.7, 39.3, 37.9, 36.7. HRMS (ESI) calcd for C₂₆H₂₄N₄O₄ [M + H]⁺ 457.1798, found 457.1872.

(S)-N1-(1-((4-methoxyphenyl)(methyl) amino)-1-oxo-3-phenylpropan-2-yl)-N2-(4-nitrophenyl)oxalamide (III-16f): white solid, yield: 57%, HPLC purity 98% ($t_R = 6.96$ min), mp: 178–180 °C. $^1\text{H NMR}$ (400 MHz, DMSO- d_6) δ 11.18 (s, 1H, NH), 9.01 (d, $J = 7.9$ Hz, 1H, NH), 8.25 (d, $J = 8.7$ Hz, 2H, PhH), 8.06 (d, $J = 8.7$ Hz, 2H, PhH), 7.24 (d, $J = 7.5$ Hz, 2H, PhH), 7.17 (t, $J = 7.1$ Hz, 3H, PhH), 7.02 (d, $J = 8.2$ Hz, 2H, PhH), 6.89 (d, $J = 6.9$ Hz, 2H, PhH), 4.56 (q, $J = 7.4, 7.0$ Hz, 1H, CH), 3.81 (s, 3H, OCH₃), 3.15 (s, 3H, NCH₃), 3.05 – 2.87 (m, 2H, CH₂). $^{13}\text{C NMR}$ (100 MHz, DMSO- d_6) δ 170.5, 159.5, 159.2, 159.1, 144.1, 143.7, 137.8, 135.8, 129.3, 128.6, 127.0, 125.1, 120.8, 115.2, 55.9, 52.7, 37.9, 36.7. EI-HRMS: m/z 477.1765 [M + H]⁺, C₂₅H₂₄N₄O₆ (476.1696).

(S)-N-(4-methoxyphenyl)-N-methyl-2-(2-(5-nitroindolin-1-yl)-2-oxoacetamido)-3-phenylpropanamide (III-16g): orange solid, yield: 56%, HPLC purity 98% ($t_R = 4.81$ min), mp: 70–72 °C. $^1\text{H NMR}$

(400 MHz, DMSO- d_6) δ 9.20 (d, J = 7.8 Hz, 1H, NH), 8.15 (p, J = 8.9 Hz, 3H, PhH), 7.21 (q, J = 8.3 Hz, 5H, PhH), 7.04 (d, J = 8.3 Hz, 2H, PhH), 6.87 (d, J = 7.0 Hz, 2H, PhH), 4.61 (d, J = 10.4 Hz, 1H, CH), 3.96 (q, J = 9.7 Hz, 1H, CH₂), 3.82 (s, 3H, OCH₃), 3.64 (q, J = 9.8 Hz, 1H, CH₂), 3.16 (s, 5H, NCH₃ + CH₂), 2.96 (dd, J = 13.9, 4.5 Hz, 1H, CH₂), 2.80 – 2.71 (m, 1H, CH₂). ¹³C NMR (100 MHz, DMSO- d_6) δ 170.6, 162.6, 162.1, 159.2, 147.8, 144.1, 137.6, 135.8, 135.1, 129.4, 129.2, 128.7, 127.0, 124.7, 121.0, 116.4, 115.3, 55.9, 51.6, 49.1, 38.7, 37.9, 27.5. HRMS (ESI) calcd for C₂₇H₂₆N₄O₆ [M + H]⁺ 503.1852, found 503.1924.

4.1.12. Synthetic route of intermediate(S)-N-(1-((4-methoxyphenyl)(methyl)amino)-1-oxo-3-phenylpropan-2-yl)-3-nitrobenzamide (17)—Intermediate **7** (0.10 g, 0.35 mmol) was dissolved in 8 mL dichloromethane, and the mixture was added triethylamine (0.07 mL, 0.53 mmol). Subsequently, 3-nitrobenzoyl chloride (0.08 g, 0.42 mmol) was added slowly to the mixture at 0°C for 4 h (monitored by TLC). Then the mixture was washed by saturated sodium bicarbonate (15 mL) and extracted with dichloromethane (3 × 8 mL). Then the combined organic phase was washed with saturated sodium chloride aqueous solution (3 × 10 mL) and was dried over anhydrous Na₂SO₄, filtered, and recrystallized with ethyl acetate and petroleum ether to afford product **17**. White solid, yield: 61%. ¹H NMR (400 MHz, DMSO- d_6) δ 9.15 (d, J = 7.8 Hz, 1H, NH), 8.68 (s, 1H, PhH), 8.37 (dd, J = 8.0, 2.3 Hz, 1H, PhH), 8.24 (d, J = 7.8 Hz, 1H, PhH), 7.76 (t, J = 8.0 Hz, 1H, PhH), 7.29 (d, J = 8.1 Hz, 2H, PhH), 7.16 (dt, J = 11.4, 6.8 Hz, 3H, PhH), 7.04 (d, J = 8.8 Hz, 2H, PhH), 6.90 (d, J = 6.9 Hz, 2H, PhH), 4.70 (dt, J = 8.3, 4.3 Hz, 1H, CH), 3.82 (s, 3H, OCH₃), 3.16 (s, 3H, NCH₃), 3.01–2.87 (m, 2H, CH₂). ESI-MS: m/z 434 [M + H]⁺, C₂₄H₂₃N₃O₅ (433.16).

4.1.13. Synthetic route of (S)-3-amino-N-(1-((4-methoxyphenyl)(methyl)amino)-1-oxo-3-phenylpropan-2-yl) benzamide (18)—Intermediate **17** (0.30 g, 0.60 mmol) was dissolved in 15 mL anhydrous ethanol. Then SnCl₂·2H₂O (0.56 g, 2.50 mmol) was added to the mixture. The resulting mixture was reacted for 8 h under nitrogen protection at room temperature (monitored by TLC). The mixture was alkalinized to pH 9 with 1 N NaOH and then filtered. The filtrate was extracted with ethyl acetate (3 × 10 mL). The combined organic phase was washed with saturated salt water (3 × 10 mL) and dried over anhydrous Na₂SO₄, filtered, concentrated under reduced pressure to give the corresponding crude product **18**. Yellow solid, yield: 88%. ¹H NMR (400 MHz, DMSO- d_6) δ 8.35 (d, J = 7.6 Hz, 1H, NH), 7.31 (d, J = 7.9 Hz, 2H, PhH), 7.16 (q, J = 10.6, 8.7 Hz, 3H, PhH), 7.06 (t, J = 8.4 Hz, 3H, PhH), 6.96 (d, J = 12.4 Hz, 2H, PhH), 6.89 (d, J = 7.1 Hz, 2H, PhH), 6.68 (d, J = 7.7 Hz, 1H, PhH), 5.19 (s, 2H, NH₂), 4.60 (q, J = 7.7 Hz, 1H, CH), 3.82 (s, 3H, OCH₃), 3.15 (s, 3H, NCH₃), 2.90 (h, J = 8.8 Hz, 2H, CH₂). ESI-MS: m/z 404 [M + H]⁺, C₂₄H₂₅N₃O₃ (403.19).

4.1.14. General procedure for the synthesis of target compounds IV-19 (a–c)—Intermediate **18** (1.0 eq) was dissolved in 15 mL dichloromethane, and the mixture was added triethylamine (1.5 eq). Subsequently, fragments containing substituted benzenesulfonyl chlorides (1.1 eq) was added slowly to the mixture at 0°C for 4 h (monitored by TLC). Then the mixture was washed by saturated sodium bicarbonate (15 mL) and extracted with dichloromethane (3 × 8 mL). Then the combined organic phase

was washed with saturated sodium chloride aqueous solution (3 × 10 mL) and was dried over anhydrous Na₂SO₄, filtered, and recrystallized with ethyl acetate and petroleum ether to afford target products **IV-19(a-c)**.

(S)-3-((4-fluorophenyl)sulfonamido)-*N*-(1-((4-methoxyphenyl) (methyl)amino)-1-oxo-3-phenylpropan-2-yl)benzamide (**IV-19a**): white solid, yield: 60%, HPLC purity 97% (*t_R* = 4.00 min), mp: 140–142 °C. ¹H NMR (400 MHz, DMSO-*d*₆) δ 10.45 (s, 1H, NH), 8.66 (d, *J* = 7.5 Hz, 1H, NH), 7.79 (dd, *J* = 8.4, 5.1 Hz, 2H, PhH), 7.51 (s, 2H, PhH), 7.38 (t, *J* = 8.5 Hz, 2H, PhH), 7.31 (d, *J* = 7.7 Hz, 3H, PhH), 7.23 (d, *J* = 8.1 Hz, 1H, PhH), 7.15 (d, *J* = 7.3 Hz, 3H, PhH), 7.05 (d, *J* = 8.3 Hz, 2H, PhH), 6.87 (d, *J* = 6.9 Hz, 2H, PhH), 4.58 (q, *J* = 7.3 Hz, 1H, CH₂), 3.83 (s, 3H, OCH₃), 3.15 (s, 3H, NCH₃), 2.89 (d, *J* = 7.3 Hz, 2H, CH₂). ¹³C NMR (100 MHz, DMSO-*d*₆) δ 171.7, 166.2, δ 164.7 (d, ¹*J*_{CF} = 251.8 Hz), 159.1, 138.5, 138.0, 136.1 (d, ³*J*_{CF} = 4.1 Hz), 135.4, 130.1, 130.0, 129.5, 129.3, 129.2, 128.5, 126.8, 123.6, 123.4, 120.3, 117.0 (d, ²*J*_{CF} = 22.9 Hz), 115.2, 55.9, 53.1, 37.9, 36.7. HRMS (ESI) calcd for C₃₀H₂₈FN₃O₅S [M + H]⁺ 562.1734, found 562.1809.

(S)-*N*-(1-((4-methoxyphenyl)(methyl)amino)-1-oxo-3-phenylpropan-2-yl)-3-((4-(trifluoromethoxy)phenyl)sulfonamido)benzamide (**IV-19b**): white solid, yield: 65%, HPLC purity 98% (*t_R* = 6.95 min), mp: 88–90 °C. ¹H NMR (400 MHz, DMSO-*d*₆) δ 10.57 (s, 1H, NH), 8.69 (d, *J* = 7.7 Hz, 1H, NH), 7.86 (d, *J* = 8.0 Hz, 2H, PhH), 7.64–7.48 (m, 4H, PhH), 7.32 (d, *J* = 8.9 Hz, 3H, PhH), 7.23 (d, *J* = 8.0 Hz, 1H, PhH), 7.15 (q, *J* = 8.3, 7.2 Hz, 3H, PhH), 7.05 (d, *J* = 8.2 Hz, 2H, PhH), 6.87 (d, *J* = 7.1 Hz, 2H, PhH), 4.57 (q, *J* = 7.3 Hz, 1H, CH), 3.82 (s, 3H, OCH₃), 3.15 (s, 3H, NCH₃), 2.88 (d, *J* = 6.8 Hz, 2H, CH₂). ¹³C NMR (100 MHz, DMSO-*d*₆) δ 171.7, 166.1, 159.1, 151.5, 138.7, 138.5, 137.9, 136.1, 135.5, 129.7, 129.5, 129.3, 129.2, 128.5, 125.2 (d, ¹*J*_{CF} = 307.4 Hz), 123.4, 121.9, 120.4, 115.2, 55.9, 53.1, 40.2, 37.8, 36.7. HRMS (ESI) calcd for C₃₁H₂₈F₃N₃O₆S [M + H]⁺ 628.1651, found 628.1727.

(S)-3-((3,5-difluorophenyl)sulfonamido)-*N*-(1-((4-methoxyphenyl) (methyl)amino)-1-oxo-3-phenylpropan-2-yl)benzamide (**IV-19c**): white solid, yield: 51%, HPLC purity 96% (*t_R* = 6.14 min), mp: 172–174 °C. ¹H NMR (400 MHz, DMSO-*d*₆) δ 10.57 (s, 1H, NH), 8.64 (d, *J* = 7.6 Hz, 1H, NH), 7.54 (t, *J* = 9.7 Hz, 1H, PhH), 7.48 (d, *J* = 7.6 Hz, 1H, PhH), 7.44 (s, 1H, PhH), 7.34 (d, *J* = 4.2 Hz, 2H, PhH), 7.29 (d, *J* = 7.9 Hz, 1H, PhH), 7.27–7.21 (m, 2H, PhH), 7.18 (d, *J* = 8.1 Hz, 1H, PhH), 7.07 (q, *J* = 8.1, 7.0 Hz, 3H, PhH), 6.97 (d, *J* = 8.2 Hz, 2H, PhH), 6.79 (d, *J* = 7.0 Hz, 2H, PhH), 4.50 (q, *J* = 7.3 Hz, 1H, CH), 3.75 (s, 3H, OCH₃), 3.08 (s, 3H, NCH₃), 2.81 (d, *J* = 7.0 Hz, 2H, CH₂). ¹³C NMR (100 MHz, DMSO-*d*₆) δ 171.7, 166.1, 162.5 (dd, ¹*J*_{CF} = 252.1, ³*J*_{CF} = 12.4 Hz), 159.1, 143.0 (t, ³*J*_{CF} = 8.3 Hz), 138.5, 137.4, 136.1, 135.6, 129.6, 129.3, 129.2, 128.5, 126.8, 124.1, 123.8, 120.7, 115.2, 110.8 (d, ²*J*_{CF} = 28.3 Hz), 109.3 (t, ²*J*_{CF} = 26.2 Hz), 55.9, 53.1, 37.9, 36.7. HRMS (ESI) calcd for C₃₀H₂₇F₂N₃O₅S [M + H]⁺ 580.1639, found 580.1713.

4.1.15. General procedure for the synthesis of intermediates 21(a–g)—Amine fragments (1.0 eq) were dissolved in 15 mL dichloromethane, and the mixture was added triethylamine (1.5 eq). Subsequently, methyl 3-(chlorosulfonyl) benzoate (**20**) (1.1 eq) was added to the mixture at 0 °C. Then the mixture was stirred for another 4 h (monitored by TLC), washed by saturated sodium bicarbonate (15 mL) and extracted with dichloromethane

(3 × 8 mL). Then the combined organic phase was washed with saturated salt water (3 × 10 mL) and was dried over anhydrous Na₂SO₄, filtered, and then the crude product were recrystallized with ethyl acetate and petroleum ether to afford intermediates **21(a–g)**.

Methyl 3-(thiomorpholine sulfonyl) benzoate (21a): white solid, yield: 68%. ¹H NMR (400 MHz, DMSO-*d*₆) δ 8.28 (d, *J* = 7.7 Hz, 1H, PhH), 8.20 (s, 1H, PhH), 8.04 (d, *J* = 7.6 Hz, 1H, PhH), 7.84 (t, *J* = 7.7 Hz, 1H, PhH), 3.91 (s, 3H, OCH₃), 3.29 – 3.14 (m, 4H, CH₂ × 2), 2.77 – 2.60 (m, 4H, CH₂ × 2). ESI-MS: *m/z* 302 [M + H]⁺, 324 [M + Na]⁺, C₁₂H₁₅NO₄S (301.04).

Methyl 3-(indole-1-ylsulfonyl) benzoate (21b): white solid, yield: 62%. ¹H NMR (400 MHz, DMSO-*d*₆) δ 8.25 (s, 1H, PhH), 8.22 (d, *J* = 7.8 Hz, 1H, PhH), 8.08 (d, *J* = 7.8 Hz, 1H, PhH), 7.75 (t, *J* = 7.8 Hz, 1H, PhH), 7.50 (d, *J* = 8.1 Hz, 1H, PhH), 7.23 (t, *J* = 7.8 Hz, 1H, PhH), 7.17 (d, *J* = 7.3 Hz, 1H, PhH), 7.01 (t, *J* = 7.4 Hz, 1H, PhH), 3.94 (t, *J* = 8.3 Hz, 2H, CH₂), 3.88 (s, 3H, OCH₃), 2.90 (t, *J* = 8.3 Hz, 2H, CH₂). ESI-MS: *m/z* 318 [M + H]⁺, 340 [M + Na]⁺, C₁₆H₁₅NO₄S (317.07).

Methyl 3-((5-methoxyindolyl)sulfonyl)benzoate (21c): white solid, yield: 68%. ¹H NMR (400 MHz, DMSO-*d*₆) δ 8.21 (d, *J* = 7.8 Hz, 1H, PhH), 8.18 (s, 1H, PhH), 7.99 (d, *J* = 7.7 Hz, 1H, PhH), 7.73 (t, *J* = 7.8 Hz, 1H, PhH), 7.42 (d, *J* = 8.7 Hz, 1H, PhH), 6.81 (d, *J* = 8.9 Hz, 1H, PhH), 6.77 (s, 1H, PhH), 3.92 (t, *J* = 8.2 Hz, 2H, CH₂), 3.88 (s, 3H, OCH₃), 3.69 (s, 3H, OCH₃), 2.75 (t, *J* = 8.2 Hz, 2H, CH₂). ESI-MS: *m/z* 347 [M + H]⁺, 369 [M + Na]⁺, C₁₇H₁₇NO₅S (347.08).

Methyl 3-((5-nitroindole-1-yl)sulfonyl)benzoate (21d): brown solid, yield: 76%. ¹H NMR (400 MHz, DMSO-*d*₆) δ 8.34 (s, 1H, PhH), 8.27 (d, *J* = 7.7 Hz, 1H, PhH), 8.20 (d, *J* = 7.9 Hz, 1H, PhH), 8.15 (d, *J* = 8.8 Hz, 1H, PhH), 8.06 (s, 1H, PhH), 7.80 (t, *J* = 8.0 Hz, 1H, PhH), 7.64 (d, *J* = 8.9 Hz, 1H, PhH), 4.08 (t, *J* = 8.5 Hz, 2H, CH₂), 3.89 (s, 3H, OCH₃), 3.12 (t, *J* = 8.5 Hz, 2H, CH₂). ESI-MS: *m/z* 363 [M + H]⁺, C₁₆H₁₄N₂O₆S (362.06).

Methyl 3-(N-(4-methoxyphenyl)-N-methylsulfonyl) benzoate (21e): white solid, yield: 62%. ¹H NMR (400 MHz, DMSO-*d*₆) δ 8.34 (s, 1H, PhH), 8.27 (d, *J* = 7.7 Hz, 1H, PhH), 8.20 (d, *J* = 7.9 Hz, 1H, PhH), 8.15 (d, *J* = 8.8 Hz, 1H, PhH), 8.06 (s, 1H, PhH), 7.80 (t, *J* = 8.0 Hz, 1H, PhH), 7.64 (d, *J* = 8.9 Hz, 1H, PhH), 4.08 (t, *J* = 8.5 Hz, 2H, CH₂), 3.89 (s, 3H), 3.12 (d, *J* = 17.0 Hz, 2H, CH₂). ESI-MS: *m/z* 336 [M + H]⁺, C₁₆H₁₇NO₅S (335.08).

Methyl 3-(N-(3,5-difluorophenyl) sulfamoyl) benzoate (21f): white solid, yield: 65%. ¹H NMR (400 MHz, DMSO-*d*₆) δ 11.02 (s, 1H, NH), 8.35 (s, 1H, PhH), 8.21 (d, *J* = 7.5 Hz, 1H, PhH), 8.08 (s, 1H, PhH), 7.77 (t, *J* = 8.0 Hz, 1H, PhH), 6.93 (t, *J* = 9.6 Hz, 1H, PhH), 6.78 (d, *J* = 8.0 Hz, 2H, PhH), 3.90 (s, 3H, OCH₃). ESI-MS: *m/z* 326 [M – H][–], C₁₄H₁₁F₂NO₄S (327.04).

Methyl 3-(N-(4-(trifluoromethyl)phenyl)sulfamoyl)benzoate (21g): white solid, yield: 71%. ¹H NMR (400 MHz, DMSO-*d*₆) δ 11.02 (s, 1H, NH), 8.36 (s, 1H, PhH), 8.19 (d, *J* = 8.0 Hz, 1H, PhH), 8.07 (s, 1H, PhH), 7.75 (t, *J* = 7.7 Hz, 1H, PhH), 7.63 (d, *J* = 8.2 Hz, 2H, PhH), 7.30 (d, *J* = 8.3 Hz, 2H, PhH), 3.89 (s, 3H, OCH₃). ESI-MS: *m/z* 358 [M – H][–], C₁₅H₁₂F₃NO₄S (359.04).

4.1.16. General procedure for the synthesis of intermediates V-25(a–j)—21(a–g) (1.0 eq) was dissolved in 10 mL THF. Then equal volume NaOH solution (2.0 eq) was added to the mixture. The mixture was stirred at room temperature for 2 h (monitored by TLC). Subsequently, the resulting mixture solution was alkalized to pH 2 with 1 N HCl and filtered to obtain the crude product **22(a–g)**. Then **22(a–g)** (1.0 eq) or commercial available **23**, **24** and PyBop (1.5 eq) was dissolved in dichloromethane. The mixture was stirred at room temperature for 0.5 h. Then DIEA (2.0 eq) and intermediates **7** was added to the mixture for another 8 h (monitored by TLC). The resulting mixture was initially washed by saturated sodium bicarbonate (15 mL) and extracted with dichloromethane (3 × 8 mL). The combined organic layer was washed by 1 N HCl and extracted with dichloromethane (3 × 8 mL). Then the combined organic phase was washed with saturated salt water (3 × 10 mL), dried over anhydrous Na₂SO₄, filtered, and recrystallized with ethyl acetate and petroleum ether to afford product **V-25(a–j)**.

(S)-3-(*N,N*-dimethylsulfamoyl)-*N*-(1-((4-methoxyphenyl)(methyl) amino)-1-oxo-3-phenylpropan-2-yl)benzamide (**V-25a**): red solid, yield: 68%, HPLC purity 97% (t_R = 4.38 min), mp: 80–82 °C. ¹H NMR (400 MHz, DMSO-*d*₆) δ 9.12 (d, J = 7.7 Hz, 1H, NH), 8.19 (s, 1H, PhH), 8.15 (d, J = 7.8 Hz, 1H, PhH), 7.89 (d, J = 7.7 Hz, 1H, PhH), 7.74 (t, J = 7.7 Hz, 1H, PhH), 7.33 (d, J = 7.7 Hz, 2H, PhH), 7.15 (q, J = 8.5, 7.2 Hz, 3H, PhH), 7.06 (d, J = 8.4 Hz, 2H, PhH), 6.90 (d, J = 6.8 Hz, 2H, PhH), 4.67 (q, J = 7.4 Hz, 1H, CH), 3.82 (s, 3H, OCH₃), 3.17 (s, 3H, NCH₃), 2.95 (d, J = 7.3 Hz, 2H, CH₂), 2.63 (s, 6H, CH₃ × 2). ¹³C NMR (100 MHz, DMSO-*d*₆) δ 171.6, 165.1, 159.1, 138.5, 136.0, 135.5, 135.1, 132.3, 130.6, 130.0, 129.3, 129.2, 128.5, 126.8, 126.7, 115.2, 55.9, 53.2, 38.7, 38.0, 36.7. HRMS (ESI) calcd for C₂₆H₂₉N₃O₅S [M + H]⁺ 496.1828, found 496.1901.

(S)-*N*-(1-((4-methoxyphenyl)(methyl)amino)-1-oxo-3-phenylpropan-2-yl)-3-(piperidin-1-ylsulfonyl)benzamide (**V-25b**): white solid, yield: 70%, HPLC purity 96% (t_R = 4.01 min), mp: 70–72 °C. ¹H NMR (400 MHz, DMSO-*d*₆) δ 9.10 (d, J = 7.6 Hz, 1H, NH), 8.15 (q, J = 8.5, 8.0 Hz, 2H, PhH), 7.86 (d, J = 7.7 Hz, 1H, PhH), 7.72 (t, J = 7.7 Hz, 1H, PhH), 7.32 (d, J = 7.9 Hz, 2H, PhH), 7.14 (d, J = 6.8 Hz, 3H, PhH), 7.05 (d, J = 8.2 Hz, 2H, PhH), 6.89 (d, J = 6.9 Hz, 2H, PhH), 4.66 (q, J = 7.0 Hz, 1H, CH), 3.82 (s, 3H, OCH₃), 3.16 (s, 3H, NCH₃), 2.94 (d, J = 7.2 Hz, 2H, CH₂), 2.89 (s, 4H, CH₂ × 2), 1.54 (s, 4H, CH₂ × 2), 1.44 – 1.29 (m, 2H, CH₂). ¹³C NMR (100 MHz, DMSO-*d*₆) δ 171.6, 165.1, 159.1, 138.5, 136.4, 136.0, 135.1, 132.2, 130.5, 130.0, 129.3, 129.2, 128.5, 126.8, 126.6, 115.2, 55.9, 53.2, 47.0, 38.7, 37.9, 25.1, 23.2. HRMS (ESI) calcd for C₂₉H₃₃N₃O₅S [M + H]⁺ 536.2241, found 536.2215. *(S)*-*N*-(1-((4-methoxyphenyl)(methyl)amino)-1-oxo-3-phenylpropan-2-yl)-3-(thio-morpholinosulfonyl)benzamide (**V-25c**): white solid, yield: 65%, HPLC purity 96% (t_R = 5.83 min), mp: 115–117 °C. ¹H NMR (400 MHz, DMSO-*d*₆) δ 9.12 (d, J = 7.6 Hz, 1H, NH), 8.17 (s, 1H, PhH), 8.14 (d, J = 7.8 Hz, 1H, PhH), 7.90 (d, J = 7.8 Hz, 1H, PhH), 7.75 (t, J = 7.7 Hz, 1H, PhH), 7.33 (d, J = 8.0 Hz, 2H, PhH), 7.16 (q, J = 8.5, 7.5 Hz, 3H, PhH), 7.06 (d, J = 8.2 Hz, 2H, PhH), 6.90 (d, J = 7.1 Hz, 2H, PhH), 4.67 (q, J = 7.6 Hz, 1H, CH), 3.83 (s, 3H, OCH₃), 3.24 (s, 4H, CH₂ × 2), 3.17 (s, 3H, NCH₃), 3.03 – 2.90 (m, 2H, CH₂), 2.69 (d, J = 6.1 Hz, 4H, CH₂ × 2). ¹³C NMR (100 MHz, DMSO-*d*₆) δ 171.6, 165.0, 159.1, 138.4, 137.1, 136.0, 135.3, 132.5, 130.2, 129.2, 128.5, 126.8, 126.4, 115.2, 55.9, 53.2, 48.2, 37.9, 36.8, 26.8. HRMS

(ESI) calcd for $C_{28}H_{31}N_3O_5S_2$ $[M + H]^+$ 554.1705, found 554.1779. (*S*)-3-(indolin-1-ylsulfonyl)-*N*-(1-((4-methoxyphenyl)(methyl)amino)-1-oxo-3-phenylpropan-2-yl)benzamide (**V-25d**): white solid, yield: 58%, HPLC purity 98% (t_R = 7.35 min), mp: 82–84 °C. 1H NMR (400 MHz, DMSO- d_6) δ 9.10 (d, J = 7.8 Hz, 1H, PhH), 8.31 (s, 1H, NH), 8.08 (d, J = 7.8 Hz, 1H, PhH), 7.91 (d, J = 7.8 Hz, 1H, PhH), 7.63 (t, J = 7.8 Hz, 1H, PhH), 7.49 (d, J = 8.0 Hz, 1H, PhH), 7.31 (d, J = 8.2 Hz, 2H, PhH), 7.16 (dd, J = 17.6, 9.4 Hz, 5H, PhH), 7.04 (d, J = 8.2 Hz, 2H, PhH), 6.97 (t, J = 7.4 Hz, 1H, PhH), 6.87 (d, J = 6.7 Hz, 2H, PhH), 4.64 (q, J = 7.5 Hz, 1H, PhH), 3.97 (dq, J = 16.9, 9.4 Hz, 2H, CH₂), 3.81 (s, 3H, OCH₃), 3.16 (s, 3H, NCH₃), 3.01 – 2.83 (m, 4H, CH₂ × 2). ^{13}C NMR (100 MHz, DMSO- d_6) δ 171.6, 164.8, 159.1, 141.4, 138.4, 136.9, 136.0, 135.1, 133.0, 132.5, 130.1, 129.3, 129.2, 128.5, 128.0, 126.8, 126.4, 126.0, 124.3, 115.2, 114.5, 55.9, 53.2, 50.5, 37.9, 36.8, 27.6. HRMS (ESI) calcd for $C_{32}H_{31}N_3O_5S$ $[M + H]^+$ 570.1984, found 570.2055.

(*S*)-3-((5-methoxyindolin-1-yl)sulfonyl)-*N*-(1-((4-methoxyphenyl)(methyl)amino)-1-oxo-3-phenylpropan-2-yl)benzamide (**V-25e**): white solid, yield: 72%, HPLC purity 96% (t_R = 6.98 min), mp: 90–92 °C. 1H NMR (400 MHz, DMSO- d_6) δ 9.07 (d, J = 7.7 Hz, 1H, NH), 8.27 (s, 1H, PhH), 8.07 (d, J = 7.6 Hz, 1H, PhH), 7.81 (d, J = 7.8 Hz, 1H, PhH), 7.62 (t, J = 7.8 Hz, 1H, PhH), 7.41 (d, J = 9.1 Hz, 1H, PhH), 7.30 (d, J = 7.9 Hz, 2H, PhH), 7.15 (d, J = 6.3 Hz, 3H, PhH), 7.04 (d, J = 8.2 Hz, 2H, PhH), 6.89 (d, J = 6.6 Hz, 2H, PhH), 6.75 (s, 2H, PhH), 4.65 (q, J = 7.5 Hz, 1H, CH), 3.97 (dq, J = 16.9, 9.6, 9.1 Hz, 2H, CH₂), 3.82 (s, 3H, OCH₃), 3.67 (s, 3H, OCH₃), 3.17 (s, 3H, NCH₃), 2.93 (d, J = 7.4 Hz, 2H, CH₂), 2.86 – 2.75 (m, 2H, CH₂). ^{13}C NMR (100 MHz, DMSO- d_6) δ 171.6, 164.9, 159.1, 156.9, 138.4, 136.8, 136.0, 135.1, 134.7, 134.6, 132.9, 130.1, 130.0, 129.3, 129.2, 128.5, 126.8, 126.5, 116.1, 115.2, 113.2, 111.5, 55.9, 55.8, 53.2, 50.8, 38.7, 37.9, 28.1. HRMS (ESI) calcd for $C_{33}H_{33}N_3O_6S$ $[M + H]^+$ 600.2090, found 600.2162.

(*S*)-*N*-(1-((4-methoxyphenyl)(methyl)amino)-1-oxo-3-phenylpropan-2-yl)-3-((5-nitroindolin-1-yl)sulfonyl)benzamide (**V-25f**): white solid, yield: 71%, HPLC purity 99% (t_R = 4.68 min), mp: 98–100 °C. 1H NMR (400 MHz, DMSO- d_6) δ 9.12 (d, J = 7.8 Hz, 1H, NH), 8.38 (s, 1H, PhH), 8.13 (t, J = 9.4 Hz, 2H, PhH), 8.06 (s, 2H, PhH), 7.70 (dd, J = 19.3, 8.5 Hz, 2H, PhH), 7.32 (d, J = 8.0 Hz, 2H, PhH), 7.12 (d, J = 6.0 Hz, 3H, PhH), 7.05 (d, J = 8.1 Hz, 2H, PhH), 6.88 (d, J = 6.5 Hz, 2H, PhH), 4.67 (q, J = 7.5 Hz, 1H, CH), 4.11 (dq, J = 18.5, 9.1 Hz, 2H, CH₂), 3.82 (s, 3H, OCH₃), 3.17 (s, 3H, NCH₃), 3.13 (d, J = 8.6 Hz, 2H, CH₂), 2.94 (d, J = 6.7 Hz, 2H, CH₂). ^{13}C NMR (100 MHz, DMSO- d_6) δ 171.5, 164.7, 159.1, 147.3, 143.6, 138.4, 136.6, 136.0, 135.3, 134.2, 133.6, 130.6, 130.1, 129.3, 129.2, 128.5, 126.8, 126.3, 124.9, 121.7, 115.2, 113.2, 55.9, 53.2, 51.3, 38.7, 37.9, 27.0. HRMS (ESI) calcd for $C_{32}H_{30}N_4O_7S$ $[M + H]^+$ 615.1835, found 615.1907.

(*S*)-*N*-(1-((4-methoxyphenyl)(methyl)amino)-1-oxo-3-phenylpropan-2-yl)-3-(*N*-(4-methoxyphenyl)-*N*-methylsulfamoyl)benzamide (**V-25 g**): yellow solid, yield: 58%, HPLC purity 96% (t_R = 6.18 min), mp: 81–83 °C. 1H NMR (400 MHz, DMSO- d_6) δ 9.06 (d, J = 7.7 Hz, 1H, NH), 8.13 (d, J = 7.7 Hz, 1H, PhH), 8.06 (s, 1H, PhH), 7.66 (t, J = 7.8 Hz, 1H, PhH), 7.57 (d, J = 7.7 Hz, 1H, PhH), 7.30 (d, J = 8.0 Hz, 2H, PhH), 7.16 (d, J = 7.0 Hz, 3H, PhH), 7.05 (d, J = 8.2 Hz, 2H, PhH), 6.98 (d, J = 8.3 Hz, 2H, PhH), 6.89 (t, J = 9.6 Hz, 4H, PhH), 4.65 (q, J = 7.5 Hz, 1H, CH), 3.82 (s, 3H, OCH₃), 3.74 (s, 3H, OCH₃), 3.17 (s, 3H, NCH₃), 3.14 (s, 3H, NCH₃),

2.94 (d, $J = 5.2$ Hz, 2H, CH₂). ¹³C NMR (100 MHz, DMSO-*d*₆) δ 171.6, 165.1, 159.1, 158.7, 138.4, 137.0, 136.0, 135.0, 133.8, 132.3, 130.5, 129.8, 129.3, 129.2, 128.6, 128.3, 126.8, 115.2, 114.6, 55.9, 55.7, 53.2, 38.7, 37.9, 36.8. HRMS (ESI) calcd for C₃₂H₃₃N₃O₆S [M + H]⁺ 588.2090, found 588.2171. (*S*)-3-(*N*-(3,5-difluorophenyl)sulfamoyl)-*N*-(1-((4-methoxyphenyl)(methyl)amino)-1-oxo-3-phenylpropan-2-yl)benzamide (**V-25h**): white solid, yield: 63%, HPLC purity 97% ($t_R = 4.37$ min), mp: 100–102 °C. ¹H NMR (400 MHz, DMSO-*d*₆) δ 10.99 (s, 1H, NH), 9.09 (d, $J = 7.7$ Hz, 1H, NH), 8.31 (s, 1H, PhH), 8.07 (d, $J = 7.8$ Hz, 1H, PhH), 7.95 (d, $J = 7.8$ Hz, 1H, PhH), 7.69 (t, $J = 7.7$ Hz, 1H, PhH), 7.30 (d, $J = 7.8$ Hz, 2H, PhH), 7.15 (d, $J = 6.9$ Hz, 3H, PhH), 7.05 (t, $J = 8.4$ Hz, 2H, PhH), 6.90 (t, $J = 9.3$ Hz, 3H, PhH), 6.77 (d, $J = 8.1$ Hz, 2H, PhH), 4.64 (q, $J = 7.7, 7.0$ Hz, 1H, CH), 3.82 (d, $J = 1.6$ Hz, 3H, OCH₃), 3.16 (s, 3H, NCH₃), 2.93 (t, $J = 10.1$ Hz, 2H, CH₂). ¹³C NMR (100 MHz, DMSO-*d*₆) δ 171.5, 165.0, 163.0 (dd, $^1J_{CF} = 245.3, ^3J_{CF} = 15.4$ Hz), 159.1, 140.7 (t, $^3J_{CF} = 13.4$ Hz), 139.6, 138.4, 136.0, 135.3, 132.6, 130.2, 129.7, 129.3, 129.2, 128.5, 126.8, 126.3, 115.2, 102.5 (d, $^2J_{CF} = 29.0$ Hz), 99.6 (t, $^2J_{CF} = 26.0$ Hz), 55.9, 53.2, 37.9, 36.8. HRMS (ESI) calcd for C₃₀H₂₇F₂N₃O₅S [M + H]⁺ 580.1639, found 580.1712. (*S*)-3-((5-aminoindolin-1-yl)sulfonyl)-*N*-(1-((4-methoxyphenyl)(methyl)amino)-1-oxo-3-phenylpropan-2-yl)benzamide (**V-25i**): yellow solid, yield: 72%, HPLC purity 99% ($t_R = 4.31$ min), mp: 95–97 °C. ¹H NMR (400 MHz, DMSO-*d*₆) δ 9.07 (d, $J = 7.7$ Hz, 1H, NH), 8.26 (s, 1H, PhH), 8.04 (d, $J = 7.7$ Hz, 1H, PhH), 7.70 (d, $J = 7.7$ Hz, 1H, PhH), 7.58 (t, $J = 7.7$ Hz, 1H, PhH), 7.31 (d, $J = 8.0$ Hz, 2H, PhH), 7.22–7.11 (m, 4H, PhH), 7.05 (d, $J = 8.3$ Hz, 2H, PhH), 6.89 (d, $J = 6.9$ Hz, 2H, PhH), 6.40 (d, $J = 8.5$ Hz, 1H, PhH), 6.31 (s, 1H, PhH), 4.93 (s, 2H, NH₂), 4.65 (q, $J = 7.5$ Hz, 1H, CH), 3.89 (dd, $J = 18.8, 9.6$ Hz, 2H, CH₂), 3.82 (s, 3H, OCH₃), 3.17 (s, 3H, NCH₃), 2.93 (d, $J = 8.4$ Hz, 2H, CH₂), 2.57 (q, $J = 8.9, 8.0$ Hz, 2H, CH₂). ¹³C NMR (100 MHz, DMSO-*d*₆) δ 171.6, 164.9, 159.1, 146.6, 138.4, 137.1, 136.0, 135.0, 134.2, 132.6, 130.8, 130.1, 129.8, 129.3, 129.2, 128.6, 126.8, 126.5, 116.8, 115.2, 113.1, 111.0, 55.9, 53.1, 50.7, 37.9, 36.8, 28.2. HRMS (ESI) calcd for C₃₂H₃₂N₄O₅S [M + H]⁺ 585.2093, found 585.2171. (*S*)-*N*-(1-((4-methoxyphenyl)(methyl)amino)-1-oxo-3-phenylpropan-2-yl)-3-(*N*-(4-(trifluoromethyl)phenyl)sulfamoyl)benzamide (**V-25j**): white solid, yield: 71%, HPLC purity 97% ($t_R = 5.55$ min), mp: 102–104 °C. ¹H NMR (400 MHz, DMSO-*d*₆) δ 10.97 (s, 1H, NH), 9.06 (d, $J = 7.7$ Hz, 1H, NH), 8.32 (s, 1H, PhH), 8.06 (d, $J = 7.6$ Hz, 1H, PhH), 7.94 (d, $J = 7.9$ Hz, 1H, PhH), 7.67 (t, $J = 7.7$ Hz, 1H, PhH), 7.61 (d, $J = 8.2$ Hz, 2H, PhH), 7.30 (d, $J = 8.2$ Hz, 4H, PhH), 7.14 (d, $J = 6.8$ Hz, 3H, PhH), 7.03 (d, $J = 8.1$ Hz, 2H, PhH), 6.89 (d, $J = 7.0$ Hz, 2H, PhH), 4.64 (q, $J = 7.4, 5.9$ Hz, 1H, CH), 3.82 (s, 3H, OCH₃), 3.16 (s, 3H, NCH₃), 3.00–2.88 (m, 2H, CH₂). ¹³C NMR (100 MHz, DMSO-*d*₆) δ 171.5, 165.0, 159.1, 141.7, 139.9, 138.4, 136.0, 135.2, 132.4, 130.1, 129.6, 129.3, 129.2, 128.5, 127.0 (q, $^3J_{CF} = 3.3$ Hz), 124.6 (q, $^1J_{CF} = 271.4$ Hz), 124.3 (q, $^2J_{CF} = 32.2$ Hz), 119.2, 115.2, 55.9, 53.1, 37.9, 36.8. ESI-MS: m/z 612 [M + H]⁺, 634 [M + Na]⁺, C₃₁H₂₈F₃N₃O₅S (611.1702).

4.2. In vitro anti-HIV assay

4.2.1. Assessment of inhibitory activity on HIV-1 replication in MT-4 cells—

Inhibitory activity of compounds against HIV-1 infection in MT-4 cells was measured as the reduction in luciferase gene expression after multiple rounds of virus infection of the cells. In brief, 200 TCID₅₀ of virus (HIV-1 NL4-3 Nanoluc-sec) was used to infect MT-4 cells (1×10^5 cells/mL) in the presence of various concentrations of compounds. The mixture

incubates at 37°C with 5% CO₂ for three days. Then the culture medium was removed from each well and 100 µL of Bright Glo reagent (Promega, Luis Obispo, CA) was added to the cells for measurement of luminescence using a Victor 2 luminometer. The effective concentration (EC₅₀) against HIV-1 strains was defined as the concentration that caused a 50% reduction of luciferase activity (Relative Light Units) compared to virus control wells.

4.2.2. Cytotoxicity assay—Parallel to the antiviral assays, MT-4 cells were cultured in the presence of various concentrations of the compounds and incubate at 37°C with 5% CO₂ for three days. Subsequently, 2, 3-bis-(2-methoxy-4-nitro-5-sulfophenyl)-2H-tetrazole-5-formylaniline of phenazine methyl sulfate (XTT) was added to the mixture. Four hours later, the absorbance was measured at 450 nm. The 50% cytotoxic concentration (CC₅₀) was defined as the concentration that caused a 50% reduction in cell viability.

4.3. Binding to CA proteins analysis via surface plasmon resonance (SPR)

Binding of **II-13c**, **V-25i**, and PF-74 was examined using a ProteOn XPR36 SPR Protein Interaction Array System (Bio-Rad) at 25 °C. ProteOn GLH sensor chips were preconditioned with two 10 s pulses of 50 mM NaOH, 100 mM HCl, and 0.5 % SDS followed by the system equilibration with the running buffer (20 mM sodium phosphate, 150 mM NaCl, and 0.005% Tween 20, pH 7.4). The surface of a GLH sensorchip was subsequently activated with a 1:100 dilution of a 1:1 mixture of 0.2 M EDC and 0.05 M Sulfo-NHS. Purified HsRAD51 was diluted to 500 µg/ml in 10 mM sodium acetate, pH 5.5, and injected immediately after chip activation across the ligand flow channels at 30 µL/min for 5 min. Unreacted protein was washed out, and the excess of unreacted ester groups on the sensor surface was capped by an injection of 1 M ethanolamine-HCl, pH 8.0, at 5 µL/min for 5 min. A reference surface to correct for nonspecific binding was similarly created by immobilizing an IgG b12 anti-HIV-1 gp120 antibody (IgG b12 anti-HIV-1 gp120; was obtained through the NIH AIDS Reagent Program, Division of AIDS, NIAID, NIH: Anti-HIV-1 gp120 Monoclonal (IgG1 b12) from Drs. Dennis Burton and Carlos Barbas). Serial dilutions of the compounds were prepared in the running buffer supplemented with 3% DMSO and injected at a flow rate of 100 µL/min for a 1 min association phase, followed by 5 min dissociation phase using the “one-shot kinetics” functionality of the ProteOn instrument. Data were analyzed with ProteOn Manager Software version 3.0 (Bio-Rad). The responses from the reference flow cell were subtracted to account for the nonspecific binding and injection artifacts. Experiments were repeated three times. The equilibrium dissociation constants (K_D) for the interactions were calculated using a one-site binding model.

4.4. Molecular dynamics simulation

The coordinate structure of capsid protein (PDB code: 5HGL), was collected from RCSB website (<https://www.rcsb.org>) for ligand–protein complex interaction analysis. The computational work performed using Schrodinger software (Schrodinger release 2020–1 license dated 20 November 2020). As crystal structure possess several structural defects such as missing hydrogen atoms, charge states, side-chain missing, loop missing, inappropriate bond order, and atomic clashes^{38,39}. These issues need to be resolved prior docking study by using protein preparation wizard. The compounds **II-13c** and **V-25i** were

also prepared by Ligprep tool prior to docking³⁹. Schrödinger suite inbuilt Epik module was also used to predict the ionization states of all compounds at pH 7 ± 2 as well as tautomers generated. This in-silico study was done under OPLS2005 forcefield.

Site specific molecular docking of both compounds against HIV-1 capsid protein performed at XP precision using the Glide module of Schrödinger suite. The Van der Waals radii scaling factor and partial charge cutoff was 0.8 and 0.15 used for docking, respectively. The binding free energy for these three complexes were also calculated by prime MMGBSA.

To validate the docking results, both complexes of compound **II-13c** and **V-25i** with capsid protein were selected for extensive 50 ns MD simulation. Both the complexes were studied for the binding stability of both compounds within their respective complex. These complexes were solvated in TIP3P water model and 0.15 M NaCl to mimic a physiological ionic concentration. The stereo-chemical geometry of 5HGL protein residues was measured by Ramachandran map by Procheck⁴⁰.

Supplementary Material

Refer to Web version on PubMed Central for supplementary material.

Acknowledgements

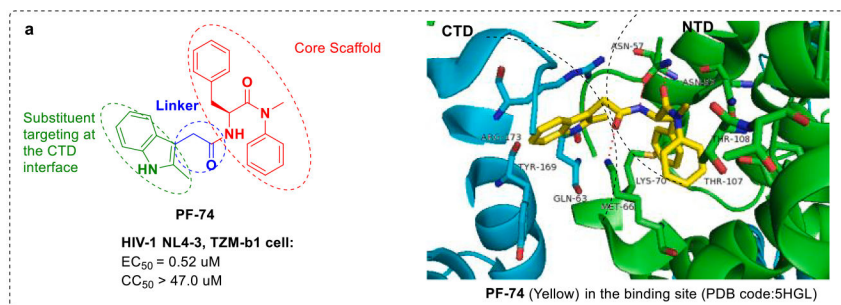
We gratefully acknowledge financial support from the the National Natural Science Foundation of China (NSFC No. 82173677), Shandong Provincial Key research and development project (No. 2019JZZY021011), Science Foundation for Outstanding Young Scholars of Shandong Province (ZR2020JQ31), Foreign cultural and educational experts Project (GXL20200015001), Qilu Young Scholars Program of Shandong University and the Taishan Scholar Program at Shandong Province, NIH grants R01GM125396 (transitioning to R01AI150491) (Cocklin, PI) and T32-MH079785 are gratefully acknowledged.

References

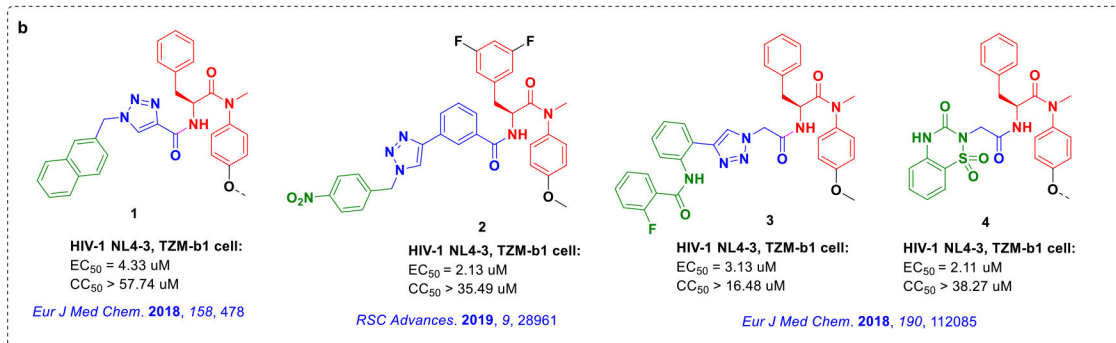
1. De Clercq E Antivirals: past, present and future. *Biochem Pharmacol.* 2013;85(6):727–744. [PubMed: 23270991]
2. Menéndez-Arias L Molecular basis of human immunodeficiency virus type 1 drug resistance: overview and recent developments. *Antiviral Res.* 2013;98(1):93–120. [PubMed: 23403210]
3. Zhang J, Crumpacker C. Eradication of HIV and Cure of AIDS, Now and How? *Front Immunol.* 2013;4:337. [PubMed: 24151495]
4. Zuo X, Huo Z, Kang D, et al. Current insights into anti-HIV drug discovery and development: a review of recent patent literature (2014–2017). *Expert Opin Ther Pat.* 2018;28(4):299–316. [PubMed: 29411697]
5. Zhou J, Price AJ, Halambage UD, James LC, Aiken C, Sundquist WI. HIV-1 resistance to the capsid-targeting inhibitor PF74 results in altered dependence on host factors required for virus nuclear entry. *J Virol.* 2015;89(17):9068–9079. [PubMed: 26109731]
6. Sundquist WI, Krausslich H-G. HIV-1 assembly, budding, and maturation. *Cold Spring Harb Perspect Med.* 2012;2(7):a006924. [PubMed: 22762019]
7. Gres AT, Kirby KA, KewalRamani VN, Tanner JJ, Pornillos O, Sarafianos SG. X-ray crystal structures of native HIV-1 capsid protein reveal conformational variability. *Science.* 2015;349(6243):99–103. [PubMed: 26044298]
8. Chen N-Y, Zhou L, Gane PJ, et al. HIV-1 capsid is involved in post-nuclear entry steps. *Retrovirology.* 2016;13(1). 10.1186/s12977-016-0262-0.
9. Thenin-Houssier S, Valente ST. HIV-1 capsid inhibitors as antiretroviral agents. *Curr HIV Res.* 2016;14(3):270–282. [PubMed: 26957201]

10. Lahaye X, Satoh T, Gentili M, et al. The capsids of HIV-1 and HIV-2 determine immune detection of the viral cDNA by the innate sensor cGAS in dendritic cells. *Immunity*. 2013;39(6):1132–1142. [PubMed: 24269171]
11. Yamashita M, Engelman AN. Capsid-dependent host factors in HIV-1 infection. *Trends Microbiol*. 2017;25(9):741–755. [PubMed: 28528781]
12. Rasaiyaah J, Tan CP, Fletcher AJ, et al. HIV-1 evades innate immune recognition through specific cofactor recruitment. *Nature*. 2013;503(7476):402–405. [PubMed: 24196705]
13. Wang W, Zhou J, Halambage UD, et al. Inhibition of HIV-1 maturation via small-molecule targeting of the amino-terminal domain in the viral capsid protein. *J Virol*. 2017;91(9). 10.1128/JVI.02155-16.
14. Campbell EM, Hope TJ. HIV-1 capsid: the multifaceted key player in HIV-1 infection. *Nat Rev Microbiol*. 2015;13(8):471–483. [PubMed: 26179359]
15. Zhang JY, Liu XY, De Clercq E. Capsid (CA) Protein as a novel drug target recent progress in the research of HIV-1 CA inhibitors. *Mini Rev Med Chem*. 2009;9(4):510–518. [PubMed: 19356128]
16. Sun L, Zhang XJ, Xu SJ, et al. An insight on medicinal aspects of novel HIV-1 capsid protein. *Eur J Med Chem*. 2021;217, 113380. [PubMed: 33751981]
17. Xu SJ, Sun L, Huang BS, et al. Medicinal chemistry strategies of targeting. *Future Med Chem*. 2020;12(14):1281–1284. [PubMed: 32483985]
18. Xu JP, Francis AC, Meuser ME, et al. Exploring Modifications of an HIV-1 Capsid Inhibitor: Design, Synthesis, and Mechanism of Action. *J Drug Des Res*. 2018; 5 (2): 1070. [PubMed: 30393786]
19. Tang C, Loeliger E, Kinde I, et al. Antiviral Inhibition of the HIV-1 Capsid Protein. *Journal of Molecular Biology*. 2003; 327 (5): 1013–1020. [PubMed: 12662926]
20. Brian NK, Sampson NK, Isaac K, et al. Structure of the antiviral assembly inhibitor CAP-1 bound to the HIV-1 CA protein. *J Mol Biol*. 2007;373(2):355–366. [PubMed: 17826792]
21. Sticht J, Humbert M, Findlow S, et al. A peptide inhibitor of HIV-1 assembly in vitro. *Nat Struct Mol Biol*. 2005;12(8):671–677. [PubMed: 16041387]
22. Lamorte L, Titolo S, Lemke CT, et al. Discovery of novel small-molecule HIV-1 replication inhibitors that stabilize capsid complexes. *Antimicrob Agents Chemothe*. 2013;57(10):4622–4631.
23. Blair WS, Pickford C, Irving SL, et al. HIV capsid is a tractable target for small molecule therapeutic intervention. *PLoS Pathog*. 2010;6(12):e1001220. [PubMed: 21170360]
24. Ganser-Pornillos BK, Cheng A, Yeager M. Structure of full-length HIV-1 CA: a model for the mature capsid lattice. *Cell*. 2007;131(1):70–79. [PubMed: 17923088]
25. Bhattacharya A, Alam SL, Fricke T, et al. Structural basis of HIV-1 capsid recognition by PF74 and CPSF6. *Proc Natl Acad Sci U S A*. 2014;111(52):18625–18630. [PubMed: 25518861]
26. Price AJ, Jacques DA, McEwan WA, et al. Host cofactors and pharmacologic ligands share an essential interface in HIV-1 capsid that is lost upon disassembly. *PLoS Pathog*. 2014;10(10):e1004459. [PubMed: 25356722]
27. Jimmy PX, Ashwanth CF, Megan EM, et al. Exploring Modifications of an HIV-1 Capsid Inhibitor Design. *J Drug Des Res*. 2018;5(2):1070. [PubMed: 30393786]
28. Kortagere S, Madani N, Mankowski MK, et al. Inhibiting early-stage events in HIV-1 replication by small-molecule targeting of the HIV-1 capsid. *J Virol*. 2012;86(16):8472–8481. [PubMed: 22647699]
29. Wu G, Zalloum WA, Meuser ME, et al. Discovery of phenylalanine derivatives as potent HIV-1 capsid inhibitors from click chemistry-based compound library. *Eur J Med Chem*. 2018;158:478–492. [PubMed: 30243152]
30. Bester SM, Wei GC, Zhao HY, et al. Structural and mechanistic bases for a potent HIV-1 capsid inhibitor. *Science*. 2020; 370(6514): 360–364. [PubMed: 33060363]
31. Jiang XY, Wu GC, Zalloum WA, et al. Discovery of novel 1,4-disubstituted 1,2,3-triazole phenylalanine derivatives as HIV-1 capsid inhibitors. *RSC Adv*. 2019; 9 (50): 28961–28986. [PubMed: 32089839]

32. Wang L, Casey MC, Vernekar SKV, et al. Novel PF74-like small molecules targeting the HIV-1 capsid protein: Balance of potency and metabolic stability. *Acta Pharm Sin B*. 2021;11(3):810–822. [PubMed: 33777683]
33. Sun L, Huang T, Dick A, et al. Design, synthesis and structure-activity relationships of 4-phenyl-1H-1,2,3-triazole phenylalanine derivatives as novel HIV-1 capsid inhibitors with promising antiviral activities. *Eur J Med Chem*. 2020;190:112085. 10.1016/j.ejmech.2020.112085. [PubMed: 32066010]
34. Jiang X, Yu Ji, Zhou Z, et al. Molecular design opportunities presented by solvent-exposed regions of target proteins. *Med Res Rev*. 2019;39(6):2194–2238. [PubMed: 31002405]
35. Xu JP, Francis JP, Meuser ME, et al. Exploring Modifications of an HIV-1 Capsid Inhibitor Design, Synthesis, and Mechanism of Action. *J Drug Des Res*. 2018;5(2):1070. [PubMed: 30393786]
36. Du J, Guo J, Kang D, et al. New techniques and strategies in drug discovery. *Chin Chem Lett*. 2020;31(7):1695–1708.
37. Na Liu, Wei L Huang Li, et al. Novel HIV-1 Non-nucleoside reverse transcriptase inhibitor agents: Optimization of diarylanilines with high potency against wild-type and rilpivirine-resistant E138K mutant virus. *J Med Chem*. 2016;59(8):3689–3704. [PubMed: 27070547]
38. Madhavi Sastry G, Adzhigirey M, Day T, Annabhimoju R, Sherman W. Protein and ligand preparation: parameters, protocols, and influence on virtual screening enrichments. *J Comput Aided Mol Des*. 2013;27(3):221–234. [PubMed: 23579614]
39. Kumar S, Sharma PP, Shankar U, et al. Discovery of New Hydroxyethylamine Analogs against 3CLpro Protein Target of SARS-CoV-2: Molecular Docking, Molecular Dynamics Simulation, and Structure-Activity Relationship Studies. *J Comput Aided Mol Des*. 2020;60(12):5754–5770.
40. Laskowski RA, MacArthur MW, Moss DS, et al. PROCHECK: a program to check the stereochemical quality of protein structures. *J Appl Cryst*. 1993;26(2):283–291.



Preliminary optimization



Scaffold hopping

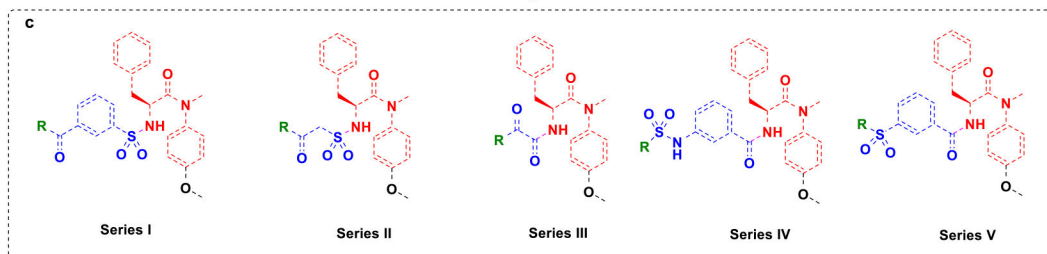


Fig. 1.

The design of novel phenylalanine derivatives as HIV-1 CA inhibitors (a) Structure and the binding mode of PF-74 in the NTD-CTD interface of CA protein hexamer (PDB code: 5HGL). Red dashed lines indicate H-bond interactions. (b) Several reported phenylalanine derivatives as HIV-1 CA protein inhibitors in our lab. (c) Target compounds designed in this work. (For interpretation of the references to colour in this figure legend, the reader is referred to the web version of this article.)

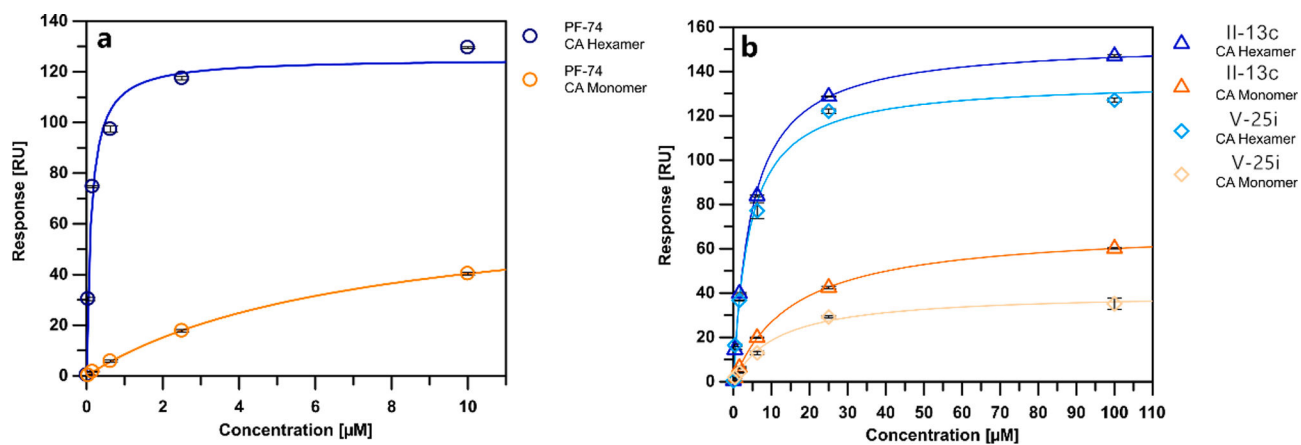


Fig. 2.
SPR isotherms of compounds **PF-74**, **II-13c** and **V-25i**.

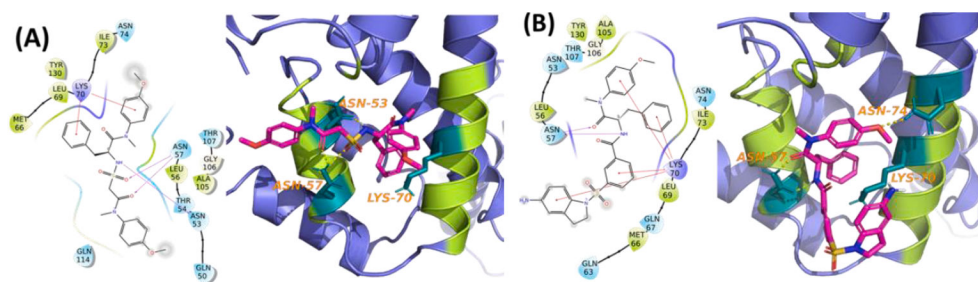


Fig. 3. Ligand-interaction to binding site residues of capsid protein (a) **II-13c**-capsid complex, (b) **V-25i**-capsid complex.

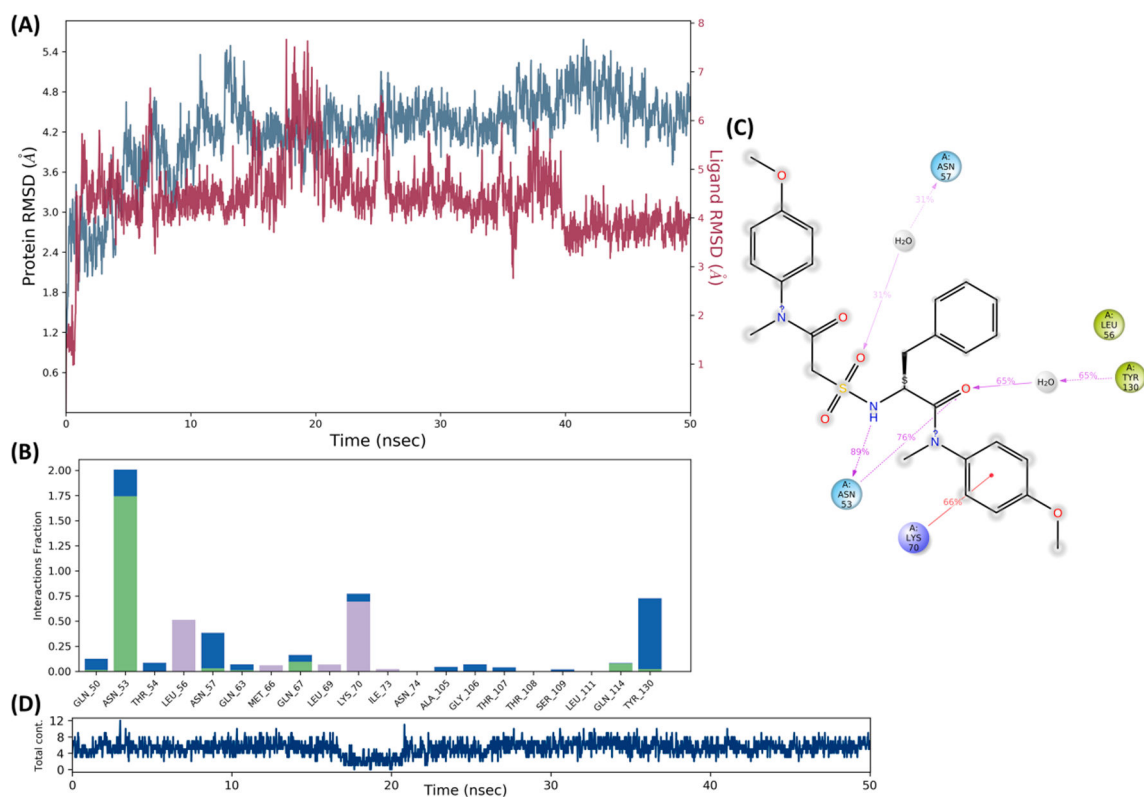


Fig. 4. Molecular dynamics and simulation of **II-13c** with capsid protein complex (a) RMSD plot for C α of capsid protein (PDB code: 5HGL) in complex with **II-13c**. (b) A Histogram plot showing residues interacting **II-13c**. (c) The percentage of interactions in molecular dynamic simulations of **II-13c** complex with capsid. (d) A timeline representation of the interactions and total contacts (H-bonds, hydrophobic interactions, ionic interactions, and water bridges) obtained during the Molecular Dynamic simulations. The panels show the total number of specific contacts the capsid made with the **II-13c** over the course of the simulation.

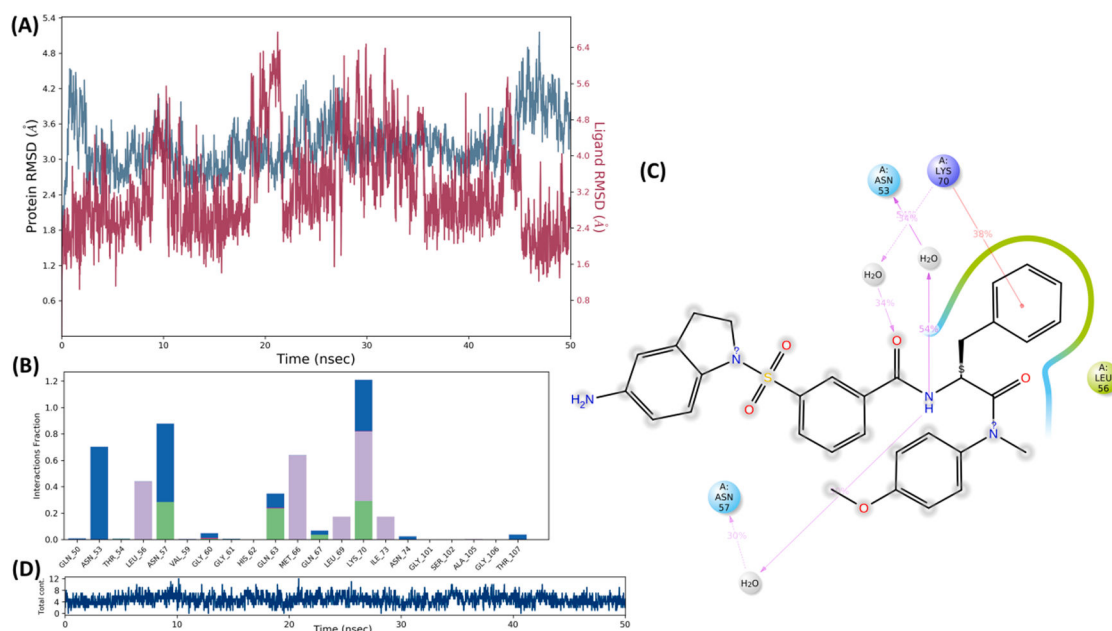


Fig. 5. Molecular dynamics and simulation of **V-25i** with capsid protein complex **(a)** RMSD plot for Ca of capsid in complex with **V-25i**. **(b)** A histogram plot showing residues interacting **V-25i**. **(c)** The percentage of interactions in molecular dynamic simulations of **V-25i** complex with capsid. **(d)** A timeline representation of the interactions and total contacts (H-bonds, hydrophobic interactions, ionic interactions, and water bridges) obtained during the molecular dynamic simulations. The panels show the total number of specific contacts the capsid protein made with the **V-25i** over the course of the simulation.

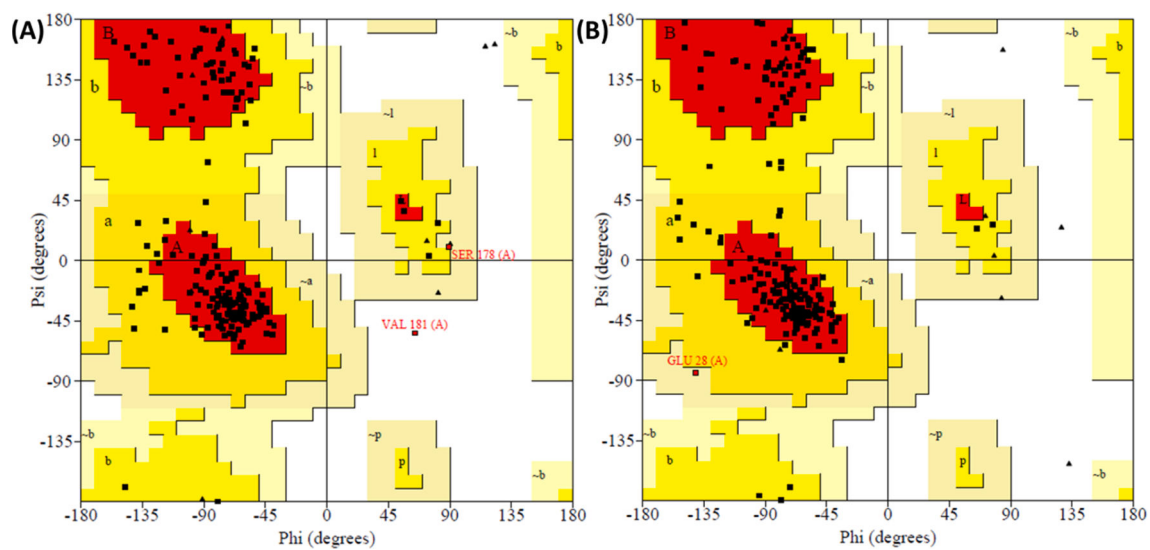
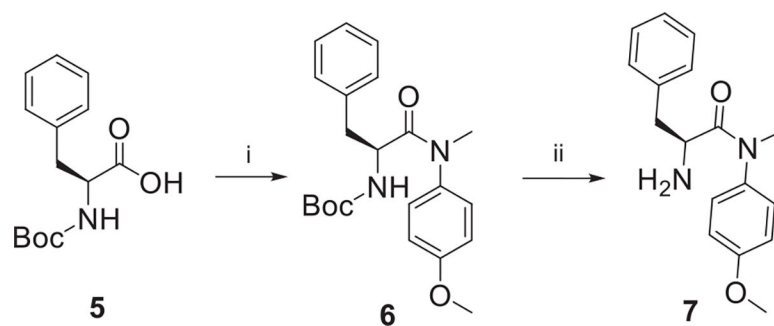
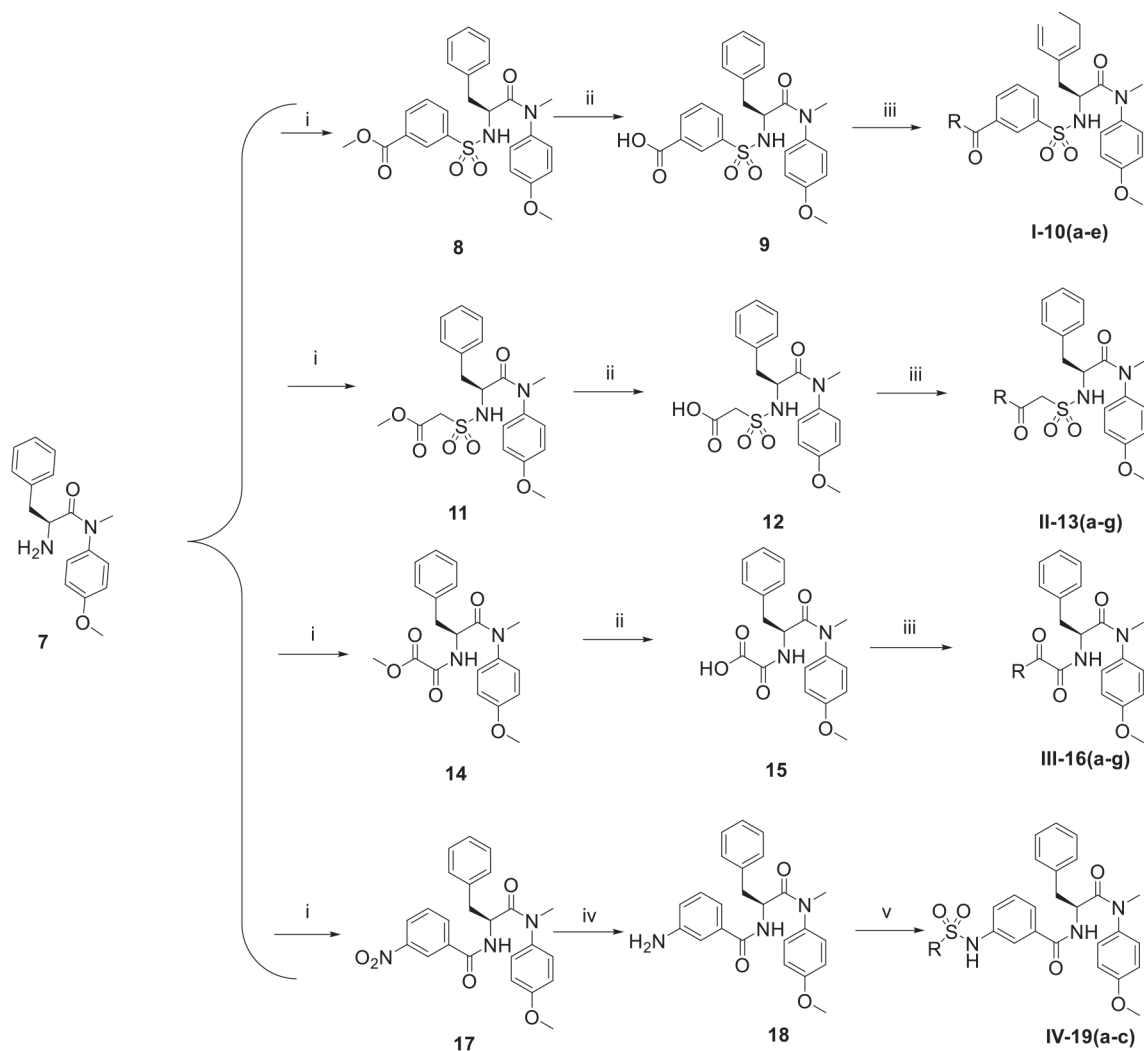


Fig. 6.
Ramachandran plot (a) II-13c-capsid complex, (b) V-25i-capsid complex.

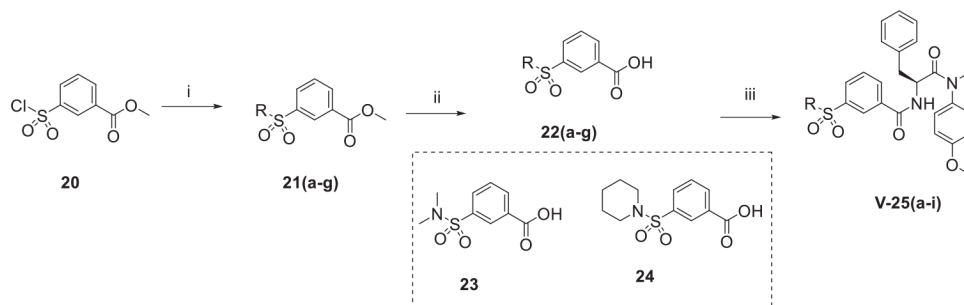
**Scheme 1.**

The synthetic route of key intermediate **7**. Reagents and Conditions: (i) 4-methoxy-*N*-methylaniline, HATU, DIEA, CH₂Cl₂, r.t., 8 h; (ii) CF₃COOH, CH₂Cl₂, r.t., 4 h.

**Scheme 2.**

The synthetic route of phenylalanine derivatives (**series I-IV**). Reagents and Conditions:

- (i) methyl 3-chlorosulfonylbenzoate or methyl 2-(chlorosulfonyl) acetate or methyl chlorooxoacetate or 3-nitrobenzoyl chloride or amine fragments, TEA, CH₂Cl₂, 0 °C, 4 h; (ii) NaOH, THF/H₂O (V:V = 1:1), r.t., 2 h; (iii) amine fragments, HATU, DIEA, CH₂Cl₂, r.t., 8 h; (iv) SnCl₂·2H₂O, EtOH, N₂, r.t., 8 h. (v) sulfonyl chloride substituents, TEA, CH₂Cl₂, 0 °C, 4 h.

**Scheme 3.**

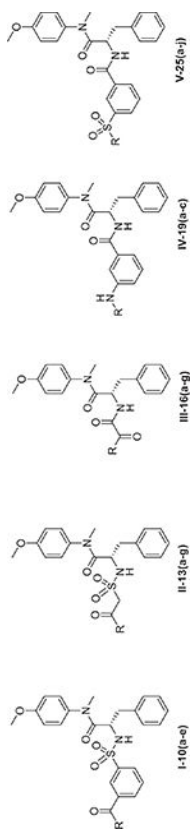
The synthetic route of phenylalanine derivatives (**series v**). (i) methyl 3-chlorosulfonylbenzoate or methyl 2-(chlorosulfonyl)acetate or methyl chlorooxoacetate or 3-nitrobenzoyl chloride or amine fragments, TEA, CH₂Cl₂, 0°C, 4 h; (ii) NaOH, THF/H₂O (V:V = 1:1), r.t., 2 h; (iii) **7**, HATU, DIEA, CH₂Cl₂, r.t., 8 h.

Author Manuscript

Author Manuscript

Author Manuscript

Author Manuscript



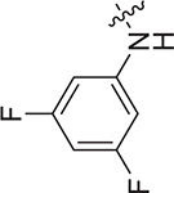
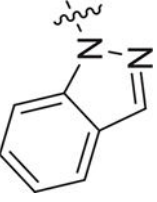
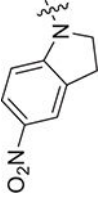
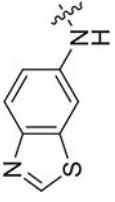
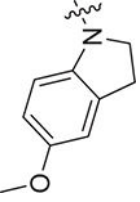
Compounds	R	EC ₅₀ ^a (μM)	CC ₅₀ ^b (μM)	SI ^c
I-10e		> 8.32	> 8.32	ND ^e
II-13a		8.09 ± 2.76	> 9.87	> 1.22
II-13b		> 9.28	> 9.28	ND ^e
II-13c		5.14 ± 1.62	> 9.51	> 1.85
II-13d		> 9.3	> 9.3	ND ^e

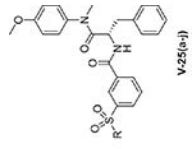
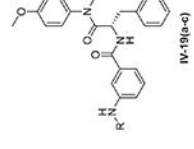
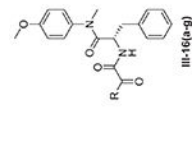
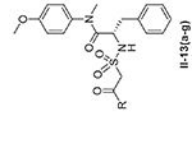
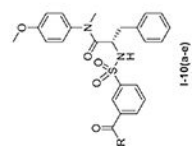
Author Manuscript

Author Manuscript

Author Manuscript

Author Manuscript

Compounds	R	EC ₅₀ ^a (μM)	CC ₅₀ ^b (μM)	SI ^c
II-13e		> 9.66	> 9.66	ND ^e
II-13f		> 9.87	> 9.87	ND ^e
II-13 g		> 9.09	> 9.05	ND ^e
III-16a		> 10.23	> 10.23	ND ^e
III-16b		> 10.26	> 10.26	ND ^e

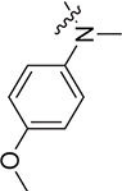
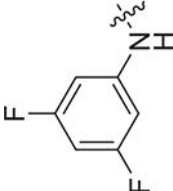
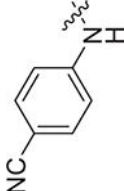
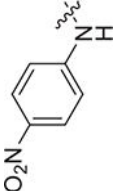
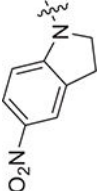


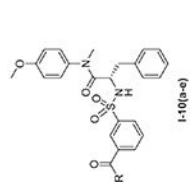
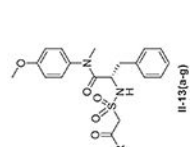
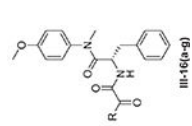
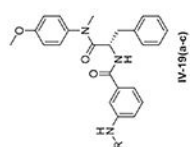
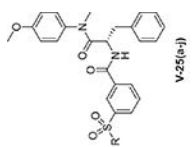
Author Manuscript

Author Manuscript

Author Manuscript

Author Manuscript

Compounds	R	EC ₅₀ ^a (μM)	CC ₅₀ ^b (μM)	SI ^c
III-16c		> 10.51	> 10.51	ND ^e
III-16d		> 8.81	> 8.81	ND ^e
III-16e		> 10.95	> 10.95	ND ^e
III-16f		> 10.49	> 10.23	ND ^e
III-16g		> 9.95	> 9.6	ND ^e

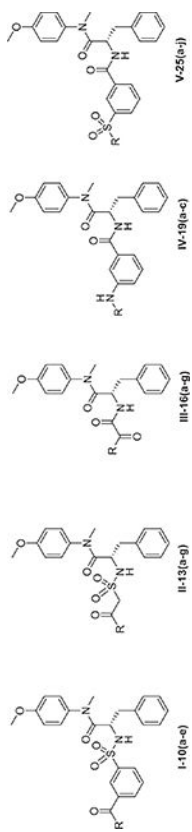


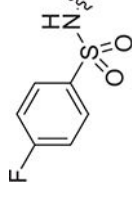
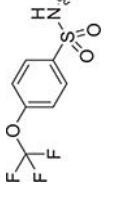
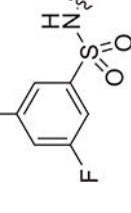
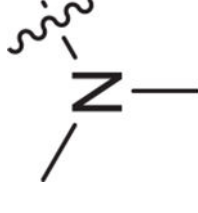

Author Manuscript

Author Manuscript

Author Manuscript

Author Manuscript



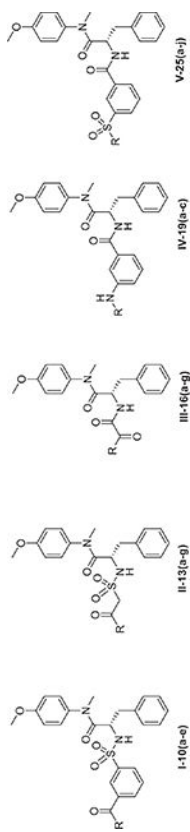
Compounds	R	EC ₅₀ ^a (μM)	CC ₅₀ ^b (μM)	SI ^c
IV-19a		> 8.91	> 8.91	ND ^e
IV-19b		> 7.97	> 7.97	ND ^e
IV-19c		> 8.63	> 8.63	ND ^e
V-25a		8.68 ± 2.62	> 10.09	> 1.12
V-25b		4.85 ± 1.53	> 9.03	> 1.86

Author Manuscript

Author Manuscript

Author Manuscript

Author Manuscript



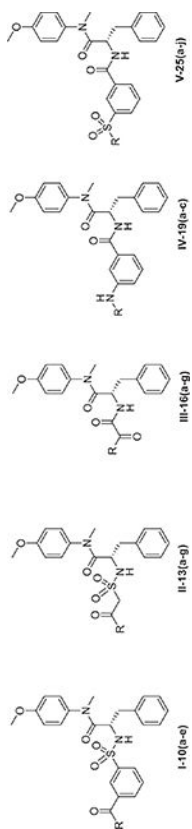
Compounds	R	EC ₅₀ ^a (μM)	CC ₅₀ ^b (μM)	SI ^c
V-25c		5.06 ± 1.43	> 9.33	> 1.84
V-25d		> 8.78	> 8.78	ND ^e
V-25e		> 8.34	> 8.34	ND ^e
V-25f		> 8.13	> 8.13	ND ^e
V-25g		5.27 ± 1.65	> 8.51	> 1.61

Author Manuscript

Author Manuscript

Author Manuscript

Author Manuscript



Compounds	R	EC ₅₀ ^a (μM)	CC ₅₀ ^b (μM)	SI ^c
V-25 h		> 8.63	> 8.63	ND ^e
V-25i		2.57 ± 0.79	> 8.55	> 3.33
V-25j		> 8.17	> 8.17	ND ^e
PF-74		0.42 ± 4.11	> 11.56	> 27.52

^dNA: No anti-HIV-1 activity or cytotoxicity at the test concentration.

^aEC₅₀: the concentration that inhibits HIV-1NL4-3 nanoluc-sec infection of MT-4 cells by 50%.

^bCC₅₀: the concentration of the compound required to reduce the viability of uninfected cells by 50%, as determined by the MTT method.

^cSI: selectivity index, the ratio of CC₅₀/EC₅₀

^eND: Not determined.

Table 2

SPR results of representative compounds and capsid proteins (hexamer, monomer).

Compds	Hexamer	Monomer
PF-74	0.12 ± 0.00 μM	7.15 ± 0.28 μM
II-13c	4.82 ± 0.30 μM	15.81 ± 0.47 μM
V-25i	4.21 ± 0.57 μM	11.62 ± 1.63 μM

Author Manuscript

Author Manuscript

Author Manuscript

Author Manuscript

Table 3

Occurance of residues in favoured, additional-allowed, generously-allowed, and disallowed region.

Entry	Complex	Residues in favoured region	Residues in additional allowed region	Residues in generously allowed region	Residues in disallowed region
1	II-13c -capsid	88.8% (166)	10.2% (19)	0.5% (1)	0.5% (1)
2	V-25i -capsid	86.6% (162)	12.8% (24)	0.5% (1)	0.0% (0)

Author Manuscript

Author Manuscript

Author Manuscript

Author Manuscript